Uptake and surface chemistry of SO2 on natural volcanic dusts

D. Urupina, J. Lasne, M.N. Romanias, Vincent Thiéry, P. Dagsson-Waldhauserova, F. Thevenet

Uptake and surface chemistry of SO_2 on natural volcanic dusts

D. Urupina[1*], J. Lasne[1], M.N. Romanias[1], V. Thiery[2], P. Dagsson-Waldhauserova[3,4], F. Thevenet[1]

(1) IMT Lille Douai, Univ. Lille, SAGE 59000 Lille, France
(2) IMT Lille Douai, Univ. Lille, GCE, 59000 Lille France
(3) Agricultural University of Iceland, Keldnaholt, Reykjavik 112, Iceland
(4) Faculty of Environmental Sciences, Czech University of Life Sciences, Prague 165 21, Czech Republic

*Corresponding author: darya.urupina@imt-lille-douai.fr

Abstract

V-dust (v-dust) is a highly variable source of natural particles in the atmosphere, and during the period of high volcanic activity it can provide a large surface for heterogeneous interactions with other atmospheric compounds. Icelandic v-dust was chosen as a case study due to frequency of volcanic eruptions and high aeolian activity in the area. In this study, we focus on the kinetics and mechanism of the reaction of sulfur dioxide (SO_2) with natural v-dust samples under atmospheric conditions using coated wall flow tube reactor and diffuse reflectance infrared Fourier transform spectroscopy (DRIFTS). Steady state uptake coefficients determined are in the range of 10^{-9} to 10^{-8} depending on the considered v-dust. Concomitantly with SO_2 uptake, both sulfites and sulfates are monitored on the surface of v-dust, with sulfates being the final oxidation product, attesting of SO_2 surface reaction. Surface hydroxyl groups play a crucial role in the conversion of SO_2 to sulfites as evidenced from both flow tube and DRIFTS experiments. Based on these experimental results, a mechanism for SO_2 interaction with different surface sites of v-dust is proposed and discussed. This study provides original insights in the kinetics of SO_2 uptake under simulated atmospheric conditions and its mechanism and transformation on volcanic material. To that regards, it brings an accurate perspective on SO_2 heterogeneous sinks in the atmosphere.

Keywords: v-dust; heterogeneous reactions; sulfur dioxide; sulfate formation; uptake coefficient; DRIFTS

1. INTRODUCTION

Volcanic eruptions comprise one of the most significant natural hazards directly threatening people living in the proximity, and, in the extreme case, can affect livelihoods of the humankind on the global scale. Large volcanic eruptions of the past have significantly influenced Earth's climate by injecting vast amounts of volcanic gases and aerosols into the atmosphere (Stevenson et al., 2003). Volcanic emissions can cause both regional and global changes to climate by affecting monsoon circulation, causing either excessive or limited rainfall thus leading to floods and droughts (Stevenson et al., 2003), (Highwood and Stevenson, 2003), ("Tambora and the 'Year Without a Summer' of 1816," 2016). Volcanic particles have an ability to affect the climate by scattering solar radiation and thus changing the Earth radiation budget (Langmann, 2013). Besides, volcanic ash, having optical and thermal properties similar to those of the black carbon, can absorb solar radiation (Arnalds et al., 2016). Vernier et al. highlighted the significance of the radiative impact of ash, in particular in the tropical latitudes due to the Brewer-Dobson circulation that sustains ash in the stratosphere for longer than was generally assumed (Vernier et al., n.d.). Finally, volcanic ash particles can affect the climate through influencing cloud formation processes and acting as ice nucleation sites during plume rise (Durant et al., 2008). The impact of v-dust on Earth's atmosphere is governed by the physical and chemical surface properties of the particles. However, the physico-chemical processes that govern the modifications of the particle surface in the plume and in the cloud when ash is in contact with volcanic gases remain poorly investigated.

Volcanic eruptions are a highly variable sources of solid particles ranging from 33 million tons (Mt) on an average year to over 100,000 Mt of ash after a major volcanic eruption, as was the case for the eruption of Mount Tambora in 1815 (Andreae, 1995). With respect to atmospheric chemistry the most significant impact would be expected to come from the particles that are in the 0.002 to 10 µm range as they can be carried over thousands of kilometers before eventually being deposited onto land or into the ocean by gravitational settling and wet deposition (Finlayson-Pitts and Jr, 1999), (Langmann et al., 2010), (Dagsson-Waldhauserova et al., 2014). When settled on land, v-dust (v-dust) can then be once again remobilized by the wind and entrained into the atmosphere. Some places on Earth are particularly prone to high aeolian

activity. Such is, for example, the case for Iceland, that experiences on average about 135 dust days per year, partly due to frequent volcanic eruptions and re-suspension of volcanic materials (Dagsson-Waldhauserova et al., 2014). In fact, this volcanic island of North Atlantic with an area of 103,000 km^2 lying south of the Arctic Circle is one of the dustiest areas of the world as well as the largest desert in Europe and the Arctic (Dagsson-Waldhauserova et al., 2014). It is also one of the most volcanically active areas. There are about 30 active volcanic systems and volcanic eruptions occurring every 3-5 years on average (Thordarson and Larsen, 2007), (Schmidt et al., 2014). Frequent dust events in Iceland transport dust over long distances, often exceeding 2,500 km, towards High Arctic (>80° N) and Europe (Ovadnevaite et al., 2009), (Groot Zwaaftink et al., 2017), (Moroni et al., 2018), (Dordevic et al., 2019). Located only 1000 km from mainland Europe, it makes a particularly interesting case study due to its proximity to densely populated European countries.

In the stratosphere, emissions of volcanic ash were linked to ozone reduction recorded after major volcanic eruptions, such as El Chichón eruption in Mexico in 1982 and Mount Pinatubo eruption in Philippines in 1991 (Brasseur et al., 1990), ("Reactions on Mineral Dust - Chemical Reviews (ACS Publications)," n.d.). Even if the effect of volcanic ash in the chemistry of the troposphere has not yet been evaluated, it is suggested that ash particles act as a long-range transporting carrier for various species adsorbed on their surface and as a solid support for their reactions with atmospheric trace gases (Li et al., 2006), (Maters et al., 2017). Some of these species are formed during eruption, when a variety of gases are released along with volcanic ash. Sulfur dioxide (SO_2) is typically the third most emitted volcanic gas after water and carbon dioxide (Durant et al., 2010). SO_2 is known to contribute to the formation of sulfuric acid aerosol, which, when injected in the stratosphere, stays there for up to 2 years effectively cooling the troposphere below (Stevenson et al., 2003), (Highwood and Stevenson, 2003).

Volcanic ash and SO_2 are likely to participate in a variety of heterogeneous reactions that could potentially influence the balance of other atmospheric species. SO_2 has already been shown to exhibit heterogeneous reactivity towards many mineral oxides such as MgO, Al_2O_3, Fe_2O_3 and TiO_2 (Usher et al., 2002). Along SO_2 uptake on these materials, sulfite and sulfate formation was detected on the surface of most mineral oxides and synthetic mineral dust and it was proposed that hydroxyl groups and surface-active oxygen are responsible for oxidation of sulfites to sulfates

(Zhang et al., 2006). Nevertheless, limited data exist on the mechanism of the interaction of SO_2 gas with natural multi-component samples, such as volcanic ash as well as on the stability of the surface species formed during reaction.

It was recently evidenced by Maters et al. that volcanic ash is reactive to the uptake of weakly acidic SO_2 gas with a reactivity that is proportional to the abundance of strongly basic sites, such as those affiliated with alkaline and alkaline earth metals (Maters et al., 2017). Although very informative of the processes occurring on the short scale, the initial uptake and the total uptake capacity measured by the authors have limited ability to explain the interactions on the longer time scale. Besides, the above-mentioned experiments were performed in a Knudsen cell under very low pressure and dry conditions that are not compliant with the atmospheric processes (Maters et al., 2017). It was therefore decided to undertake a comprehensive study of the interactions of SO_2 with v-dust under atmospheric conditions. Iceland was chosen as a location of interest for sample collection required to study heterogeneous reactivity of volcanic ash and SO_2 gas. The scope of this study is threefold. First, different natural volcanic and Icelandic samples were collected and characterized using various techniques, such as SEM (Scanning Electron Microscopy) and ICP-MS (Inductively Coupled Plasma-Mass Spectrometry). Second, the uptake of atmospheric SO_2 by the surface of selected v-dusts was investigated using a flow tube reactor. Finally, Diffuse Reflectance Fourier Transformed Spectroscopy (DRIFTS) employed for the *in-situ* monitoring of adsorbed phase was used to identify the surface species formed and to clarify the surface reaction mechanisms. The *in-situ* spectroscopic approach has been complemented by HPLC (High-Performance Liquid Chromatography) technique employed for quantification of the surface products.

2. EXPERIMENTAL SECTION

2.1 Materials

2.1.1 Origin of the dust samples

All five samples of v-dust come from different dust hot spots of Iceland. The properties of Hagavatn (64°28´6,12"N 20°16´55,81"W), Mýrdalssandur (63°26'50.1"N 18°48'52.8"W), Maelifellssandur (63°48'48.7"N 19°07'42.5"W) and Dyngjusandur (64°50'41,885"N 16°59'40,78"W) v-dusts are described by Arnalds et al. (Arnalds et al., 2016). Overall, these areas are subjected to extremely large aeolian erosion due to frequent dust storms, and have extensive

areas (10 to 140 km^2), hence providing a large supply (31-40 million tons annually) of v-dust to the atmosphere. Samples were collected from the top surface layer of each dust hot spot. The samples were dry and did not come in contact with soil or other organics. The fifth sample of Eyjafjallajökull (63°33'50.4"N 19°27'28.8"W) volcanic ash was collected and stored dry during the second phase of the explosive-effusive volcanic eruption on April 27. It is a typical volcanic ash sample as characterized by Gislason et al. (Gislason et al., 2011).

2.1.2 Characterization of the samples

Scanning Electron Microscopy / Morphology of the samples was analyzed by SEM carried out on a Hitachi S-4300SE/N SEM in high vacuum mode. The images of different v-dust particles are presented in Figure 1. These are small particles with rough edges. Dust from Eyjafjallajökull (Figure 1e) has larger particle size with many particles reaching 500 µm in diameter, while the other four dusts (Figure 1a-d) have a much finer structure and range from 10 to 50 µm in diameter due to glaciofluvial processes leading to their generation.

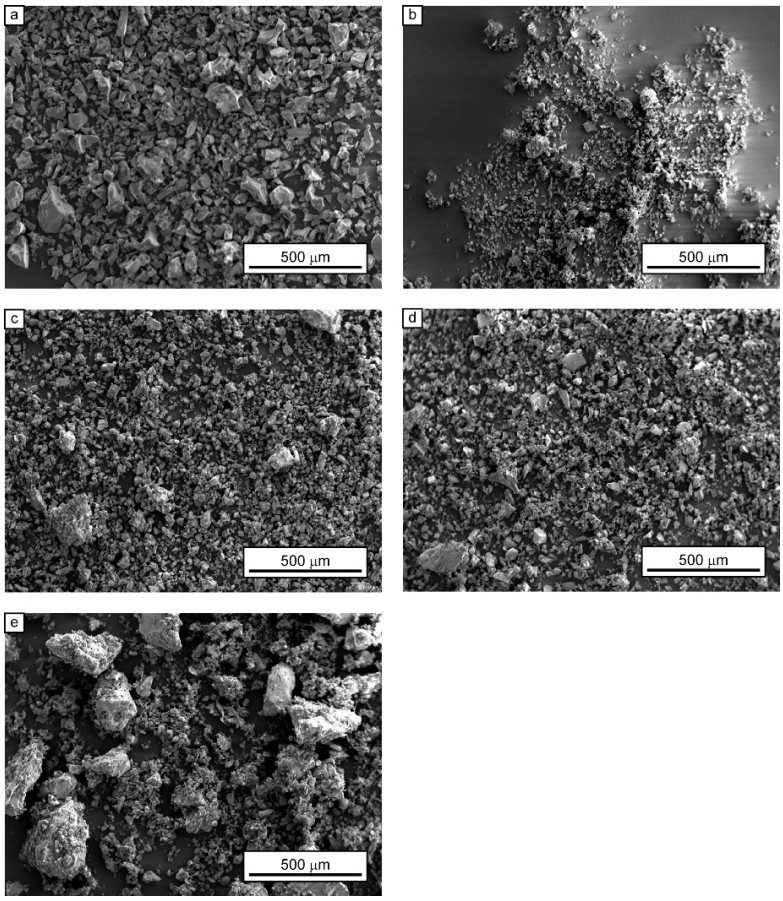

Figure 1: SEM images of five v-dusts: (a) Mýrdalssandur, (b) Dyngjusandur, (c) Hagavatn, (d) Maelifellsandur, (e) Eyjafjallajökull.

Specific surface area measurements / To avoid any overestimation of the uptake coefficients by the use of the geometric surface of the sample bed, it was decided to use the specific surface area (*SSA*) in the uptake calculations as discussed in the latest IUPAC evaluation (Crowley et al., 2010). In brief, the determination of the uptake coefficient using the geometric surface - i.e. the geometric area of the tube covered with the volcanic dust as noted in equation 2 (see section 2.2.1) of the manuscript- overestimates the uptake since it does not consider all the surface of the dust as accessible to gaseous SO_2. However, in a series of experiments it was evidenced that the entire surface area of the sample is accessible to the gas environment and thus the total surface area of the dust deposited in the tube should be used to determine the real uptake coefficient. The *SSA* is a physical property of solids, which represents the total surface area of a material per mass unit ($m^2\ g^{-1}$), and is used for the determination of the kinetic and sorption parameters (see section 2.2.1). To determine *SSA*, the Brunauer–Emmett–Teller (BET) method was employed. Nitrogen (N_2) adsorption measurements were performed with a laboratory gas sorption analysis system

(Joshi et al., 2017), (Ibrahim et al., 2018) within 0.05 to 0.3 relative pressure range (P/P_0) of N_2. To determine the range of uncertainty, three adsorption measurements were conducted for each sample. The results of the BET specific surface area (SSA_{BET}) of the 5 samples are displayed in Table 1.

Origin of the Icelandic v-dust sample	BET Specific Surface Area ($m^2\ g^{-1}$)
Mýrdalssandur	1.5 ± 0.38
Dyngjusandur	7.0 ± 1.8
Hagavatn	4.5 ± 1.1
Maelifellssandur	8.2 ± 2.0
Eyjafjallajökull	0.75 ± 0.19

Table 1: BET Specific Surface Area of the v-dust samples used in this study.

Chemical composition / The bulk elemental composition of the samples of Icelandic v-dust used in this study was determined by ICP-MS using a Perkin Elmer NeXion 300x spectrometer, the results are presented in Table 2. Prior to the analysis, from 2 to 7 mg of each sample were treated in a mixture of acids ($HF/HNO_3/H_2O_2$) in a microwave oven (Milestone Ultrawave) at 500 K and 35 bar for 15 min (Alleman et al., 2010). Six measurements per sample were performed to evaluate their chemical heterogeneity. Repeated measurements were carried out on acid blanks, quality control standard solutions and standard reference material (NIST SRM 1648a and SRM 2584) to evaluate detection limits, accuracy and to validate the whole procedure. As can be seen from Table 2 silicon is the most abundant element of the v-dust, followed by iron, calcium, and aluminum. Within the five selected v-dust samples the elemental composition seems to differ only slightly, except for Eyjafjallajökull v-dust which exhibits a higher amount of silicon than other samples and a lower amount of calcium, iron and magnesium. The results of ICP-MS analysis for Eyjafjallajökull v-dust agrees well with the literature (Gislason et al., 2011). The difference in the composition of Eyjafjallajökull v-dust in comparison with other samples is most probably due to the difference in the composition of magma that produced it. Indeed, the volcanic systems that supply Dyngjusandur dust hotspot (Bárðarbunga and Kverkfjöll volcanic systems) and Mýrdalssandur and Maelifellssandur dust hotspots (Katla volcanic system) have magmas of a predominantly basaltic composition, while magma of Eyjafjallajökull is andesitic, meaning that it is higher in silicon ("Icelandic Volcanoes," n.d.), (Vogel et al., 2017). The decrease of calcium, iron and magnesium with increasing silicon content is in accordance with the expected variation

of the composition of magma (Vogel et al., 2017). Other processes that can influence the composition of magma during a particular eruption include crystallization (Clague and Denlinger, 1994), melting of the crustal rocks (Deegan, 2010) and mixing of original magma with another magma that evolved separately ("Icelandic Volcanoes," n.d.). Since composition of magma can change within the same eruption, one might expect to see different compositions of v-dust both on the time scale and on the location scale. Transported dust can also have a different composition further away from the source. Globally, when compared to other types of mineral dusts, such as Saharan dusts or Gobi dust (Joshi et al., 2017), the amount of silicon in all five v-dust samples is considerably lower while the amount of iron, magnesium, and titanium is higher (Romanias et al., 2016), (Langmann, 2013).

Element	Mýrdalssandur	Dyngjusandur	Hagavatn	Maelifellssandur	Eyjafjallajökull	Bordj Saharan dust (Joshi et al., 2017)	Gobi dust (Joshi et al., 2017)
Si	**31.3 ± 2.2**	**32.7 ± 2.0**	**27.5 ± 2.8**	**28.3 ± 2.4**	**49.5 ± 0.9**	**94.4**	**57.6**
Fe	**23.0 ± 1.5**	**19.7 ± 0.2**	**19.6 ± 0.7**	**23.8 ± 0.8**	**13.0 ± 0.5**	**1.3**	**5.5**
Ca	**13.9 ± 1.3**	**16.3 ± 0.3**	**19.5 ± 1.1**	**14.0 ± 0.3**	**7.3 ± 0.1**	**1.0**	**16.1**
Al	**12.3 ± 3.1**	**15.8 ± 0.2**	**16.7 ± 3.2**	**15.5 ± 0.1**	**13.6 ± 0.9**	**1.8**	**11**
Mg	**5.1 ± 1.2**	**7.3 ± 0.1**	**10.4 ± 1.8**	**5.7 ± 0.4**	**3.3 ± 0.2**	**0.1**	**2.3**
Ti	**7.6 ± 0.7**	**3.3 ± 0.4**	**2.4 ± 0.1**	**6.1 ± 0.4**	**2.4 ± 0.1**	**0.7**	**0.8**
Na	**4.8 ± 0.2**	**3.9 ± 0.1**	**3.1 ± 0.1**	**4.6 ± 0.1**	**7.3 ± 0.3**	**0.2**	**2.5**
K	**1.3 ± 0.2**	**0.6 ± 0.1**	**0.2 ± 0.1**	**1.5 ± 0.1**	**3.1 ± 0.1**	**0.1**	**3.5**
other	**0.7**	**0.4**	**0.6**	**0.5**	**0.5**	**0.1**	**0.7**

Table 2: % elemental composition of the v-dust samples used in this study and of mineral dust samples adopted from (Joshi et al., 2017), as determined by ICP-MS experiments.

2.1.3 Gases

Experiments are carried out using zero air; it is generated by a classical air compressor, and then passed through a catalytic zero air generator (Claind ZeroAir 2020, Lenno, Italy) coupled to a swing adsorption (PSA) device. The remaining impurity levels in the air stream before entering the reactor are lower than the analytical system detection limits: VOCs < 0.1 ppb, CO_2 < 10 ppb, and CO < 80 ppb. Moisture level is ca. 2 ppm. In experiments requiring humid air, a second flow of zero air going through a bubbler of ultrapure water (milli-Q, resistivity 18.2 MΩ cm) is mixed with the dry air flow, in proportions necessary to reach the relative humidity (*RH*) targeted. Certified gas cylinders are used as SO_2 source. For low concentration experiments aiming to determine uptake coefficients in the flow tube, an SO_2 cylinder of 8.96 ppm in air (20.7 % O_2, 79.3 % N_2) provided by "Air Liquide" is used. Regarding the mechanistic investigation

employing DRIFT spectroscopy, higher concentrations are used and a certified cylinder of 250 ppm (Messer, France) diluted in synthetic air (nearly 80% N_2 and 20% O_2) is the SO_2 source.

Throughout the manuscript, gas concentrations are given in ppmv and ppbv (parts per million and parts per billion by volume, respectively). Under usual experimental conditions (T = 296 K, P = 1 atm), the conversion to a concentration is given by 1 ppbv (SO_2) ≈ 2.5×10^{10} molecules cm^{-3}. Note that this conversion factor takes a different value when the temperature or total pressure changes.

2.2 Experimental set ups

2.2.1 Coated wall flow tube reactor

The heterogeneous interaction of SO_2 with v-dust was investigated in a horizontal double wall flow tube reactor represented schematically in Figure 2. The experiments were conducted under relevant atmospheric conditions, i.e. SO_2 concentration in the ppb range, atmospheric pressure, room temperature, under dry conditions and 30% *RH*. The objective of this series of experiments was to determine the uptake coefficients of SO_2 on the various Icelandic v-dusts.

The setup was described in detail in a previous paper (Lasne et al., 2018) it mainly consists of three parts; (i) the gas mixing line, (ii) the reactor and (iii) the analytical device. The gas preparation line is used for the mixing of zero dry/humid air with SO_2 resulting in a flow with the desired proportion of *RH* and SO_2 concentration. The reactor is made of a double wall Pyrex glass and is thermostated by circulating water in between the double wall surrounding the flow tube. Inside and along the axis of the reactor, a Pyrex tube covered on its inner wall with the v-dust is introduced. To coat the inner surface of a Pyrex tube with v-dust (orange color in Figure 2), a defined mass of dust is first inserted in a tube. A small amount of water is added to form a slurry and the tube is shaken to deposit an even coating on the Pyrex surface. Then, the tube is heated slightly above 380 K for 10 minutes to evaporate excess water, placed in the reactor and flushed overnight with dry air. Potential modifications of the volcanic dust upon its dissolution in water in the process of slurry preparation and subsequent drying process include displacement of soluble salts that might be found on the surface of v-dust particles as well as leaching of alkali and alkaline earth metals from the aluminosilicate network at ash surfaces (Witham et al., 2005). In the case of Hagavatn, Mýrdalssandur, Maelifellssandur and Dyngjusandur natural v-dust samples, that were likely previously exposed to water the above mentioned phenomena does not seem to effect the results because the soluble salts would be expected to leach out by the time of

239 the experiment. In the case of fresh Eyjafjallajökull dust leaching of the soluble salts formed
240 during ash-gas interaction in the plume presents a valid concern. In order to minimize removal of
241 soluble salts the amount of water added to prepare a slurry was as small as necessary to spread
242 the dust evenly, i.e. in the case of Eyjafjallajökull 1:3 ash (g) to water (mL) ratio was used, which
243 is much smaller than the 1:25 ash-to-water ratio recommended for preparation of ash leachates
244 (Witham et al., 2005). In addition, contact time with water was minimized to around 10 seconds
245 shaking followed by rapidly drying the slurry, which is also much faster than 90 min agitation
246 procedure recommended by Witham et al. (Witham et al., 2005). One could also expect that
247 drying the slurry would lead to redisposition of the displaced salts, even though some of it could
248 be redeposited on the surface of the glass tube and not the v-particles. Two Viton O-rings are
249 placed around the Pyrex tube to fix its position inside of the reactor. The gas mixture is flowed
250 through a movable injector (internal diameter of 0.3 cm) with a flow rate ranging between 250
251 and 500 sccm, ensuring laminar flow conditions with a Reynolds number, $R_e < 50$. The role of
252 the moveable injector is to either isolate (placed at the downstream end of the flow tube) or to
253 expose the dust surface to the gas environment (upstream end of the reactor). The outgoing flow
254 is then directed to the SO_2 analyzer (Model 43C, Thermo Environmental Instruments Inc.) for the
255 real time gas phase monitoring of SO_2, with a time resolution of 10 seconds. We didn't noticed
256 any loss of dust during the uptake experiments. Note that the tubes with the deposited dust are
257 weighted before and after the experiments and the variations noticed were in the range of the mass
258 scale uncertainty (<1%). In addition, considering that the flow rate during the experiments is
259 relative slow, the experiments are carried out under atmospheric pressure and no pressure
260 variation takes place between the reactor and the analyzer, it is highly improbable to experience
261 any loss of dust during our measurements. Furthermore, we have not observed (at least visually)
262 any large particles to fail to adhere to the Pyrex tube. However, even if this was the case, in the
263 horizontal flow tube, these particles would still be subjected to the flow of gas and thus remain
264 accessible to the gas. To conclude, the total mass of the dust inside the reactor is maintained
265 during the entire experiment and is accessible to the gas environment and hence the total surface
266 area does not change and no correction is required to determine the uptake coefficients. The
267 uptake of SO_2 by v-dust is studied under dark conditions at $T = 296$ K, $[SO_2] \approx 75$ ppb ($1.88 \times$
268 10^{12} molecules cm^{-3}) in air, and a relative humidity of either 30 % or under dry conditions (i.e.
269 $RH < 0.1$ %). Regarding RH, studying the uptake under dry conditions provides an evaluation of

the interaction of the probe gas with the direct surface of volcanic material, while increasing *RH* to 30% contributes to the understanding of the impact of the water coverage on the mineral aerosol (Joshi et al., 2017).

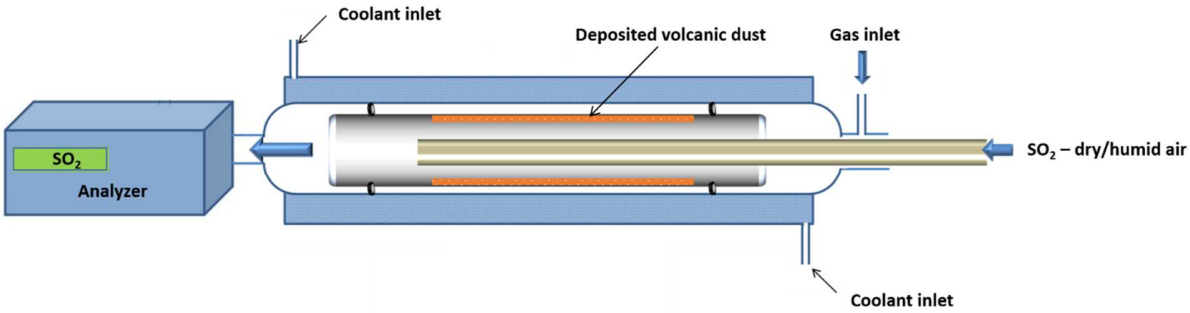

Figure 2: Schematic representation of the Coated wall Flow Tube (CWFT) reactor used in this study. The space filled with the coolant in between the two walls is shaded in blue. The dust sample coating the inner surface of the Pyrex tube is shown in orange.

Theoretical SO_2 concentration profile is represented in Figure 3. During a typical flow tube experiment SO_2 is flowed through the reactor, the dust being left unexposed initially. After a stable SO_2 concentration, $[SO_2]_0$, is set, the injector is pulled out and the dust is exposed to SO_2; the change in SO_2 concentration related to its uptake by dust is recorded by the SO_2 analyzer. After a steady-state is reached, the injector is pushed back in to control the $[SO_2]_0$. What is obtained as a result of the flow tube experiment is a time evolution of the trace gas concentration at the tube exit, the so-called breakthrough curve, that is used to calculate the steady state uptake coefficient (Huthwelker et al., 2006). In the case of SO_2 a long-lasting tailing of the breakthrough curve is observed, similar to the one described for the uptake of nitric acid (HNO_3) on ice (Huthwelker et al., 2006). This phenomena leads to the following question: at which point can we say that a steady state is reached? In the absence of the generally accepted understanding of the nature of tailing and for the practical reasons the following pragmatic approach was adopted. Steady state is considered to be reached when the variation of the signal falls within 1.5% of its value for at least three hours. On average it takes about 12 hours to reach the steady state under 30% humidity, which is much longer than 1 hour needed to achieve a steady-state for the uptake of ozone by clay dust (Lasne et al., 2018).

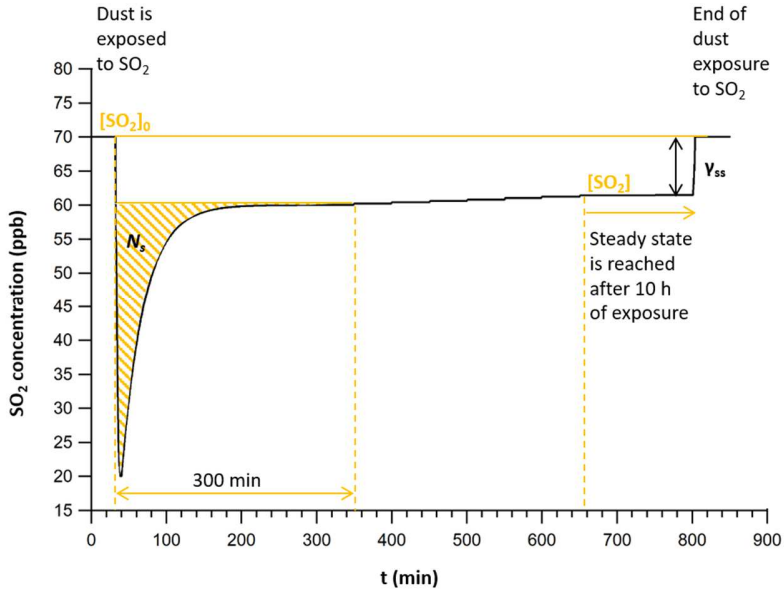

Figure 3: Theoretical SO_2 concentration profile during a typical flow tube experiment with v-dust exposed to SO_2. At the beginning of the experiment where surface is isolated from the gas mixture the initial SO_2 concentration is $[SO_2]_0$, then the dust is exposed to the gas and the concentration of SO_2 falls to its minimum, after which it recovers till a steady-state is reached. Note that the steady-state concentration $[SO_2]$ is different from the initial state concentration $[SO_2]_0$. Initial concentration is controlled when the injector is pushed in and the SO_2 gas in no longer in contact with the dust. Shaded area corresponds to the integrated area that is used to obtain the number of molecules during the transient initial uptake of SO_2 on v-dusts N_s (molecules cm^{-2}). 300 min was chosen as integration limits for the determination of N_s.

Preliminary experiments were conducted to determine a possible contribution of the Pyrex surfaces to the uptake of SO_2. They showed negligible contribution to the parameters determined in the current study.

The measurements of $[SO_2]$ at steady-state and at the initial level, $[SO_2]_0$, together with the knowledge of the parameters defining our setup are necessary to conduct the analysis leading to the determination of the uptake coefficients under equilibrium conditions, γ_{ss} (Lasne et al., 2018). Assuming first order kinetics for the uptake of SO_2 by v-dust surfaces, the observed constant of reaction, k_{obs} (in s^{-1}), is determined by (1):

$$k_{obs} = \frac{v}{L} \times \ln\left(\frac{[SO_2]_0}{[SO_2]}\right) \quad (1)$$

where v is the flow in the reactor (in cm s^{-1}) and L is the length of the dust coating (in cm). The value of k_{obs} (in s^{-1}) is corrected for diffusion of SO_2 with a constant k_{diff} (in s^{-1}) to give the diffusion-corrected constant k_{kin} (in s^{-1}). In this work, a diffusion coefficient of SO_2 in the air derived from (Massman, 1998) is used, D(296 K) = 95.28 Torr cm^2 s^{-1}. This value is in excellent

agreement with D = 94 ± 13 Torr cm^2 s^{-1} suggested by Tang et al (Tang et al., 2014). The diffusion-corrected constant, k_{kin}, is then used to determine γ_{ss}, (2):

$$\gamma_{ss} = \frac{4k_{kin}V}{cS_{geom}} \quad (2)$$

where V and S_{geom} are the volume (in cm^3) and geometric surface (in cm^2) of the region where the reaction takes place, respectively, and c is the average molecular speed (in cm s^{-1}). The diffusion-correction accounts for *ca.* 5 % of the measured uptake coefficients.

A series of experiments were carried out as a function of Mýrdalssandur v-dust mass deposited that showed a linear increase in the 0 - 250 mg range. The linear increase of the uptake with mass and the lack of saturation reflect the fact that the entire surface of the dust is accessible to SO_2 molecules from the gas and thus the specific surface area SSA_{BET} is used for the calculation of the uptake coefficient, $\gamma_{ss,BET}$, (3):

$$\gamma_{ss,BET} = \gamma_{ss} \times \frac{S_{geom}}{A_s} \quad (3)$$

where A_s, is the effective surface area of the dust, obtained from multiplying SSA_{BET} (m^2 g^{-1}) by the mass of the sample (g).

The error on the uptake coefficients is the root-mean-square deviation of the values measured. It was calculated with the precision of the signal (0.5% of the measured concentration) and its propagation to k_{obs} measurement, the *SSA* determination (~ 25%) and all relevant uncertainties, i.e. on the gas flow measurement, temperature, mass weighting, and length of the exposed dust coating (~8%). The total error calculated for the γ values was estimated to be ca 35% in all experiments and a safe limit of 40% is given. Although the quoted uncertainty is significant, it reflects the real error accounted for the measurement of slow uptake processes (uptakes on the order of 10^{-9}) in the flow tube.

Besides uptake coefficients, the transient initial number of SO_2 molecules taken up per surface area of v-dusts N_s (molecules cm^{-2}) is determined at 30% of *RH*; by integrating the area of the initial uptake process in a typical uptake experiment (Figure 3) divided by the effective surface area of the dust, A_s, according to (4):

$$N_s = \int_{\tau=0}^{\tau=t} \frac{F_t}{A_s} d\tau \quad (4)$$

where F_t is the flow rate (molecules min^{-1}) of SO_2 molecules through the reactor. The total error in N_s determination is estimated to be ca. 30% and includes all systematic uncertainties and the error in *SSA* determination.

It should be noted that since the SO_2 concentration recorded at the steady-state was lower than its pre-exposure concentration, for the determination of N_s solely the transient initial uptake removal of SO_2 is considered (dashed area in Figure 3). The long tailing of the breakthrough curve observed points to additional physico-chemical processes besides the absorption/desorption. Therefore for the determination of integration parameter a similar to two-third criterion approach was adopted as recommended by Huthwelker et al., where "the surface uptake is considered finished once the breakthrough curve rises to two-thirds of its initial value" (Huthwelker et al., 2006). The integration limits for the determination of the number of molecules N_s were chosen from the time of the exposure of SO_2 to the dust to 300 min after the exposure to make sure that the change in the breakthrough curve towards steady state has occurred for all the dusts. This criterion was adopted in order to be able to compare the uptake capacity of the v-dusts at the initial stage of the interaction with SO_2. On longer scale, samples can be compared based on the $\gamma_{ss,BET}$ values.

2.2.2 DRIFTS experiments

The heterogeneous interaction between SO_2 gas and v-dusts was studied *in-situ* inside of the optical DRIFTS cell operated at atmospheric pressure and room temperature under dry and 30% *RH* conditions. The objective of this series of experiments was to monitor the adsorbed species formed on the surface of v-dusts, aiming to elucidate the mechanism of the interaction under both dry and humid conditions.

The DRIFT experimental setup consists of three parts: (i) the gas supply line, (ii) the optical reactor, and (iii) the analytical device as described previously by Romanias et al. (Romanías et al., 2016). A representation of the system is given in Figure 4. The heterogeneous reactions between SO_2 and different v-dust samples are monitored *in situ* inside of the optical DRIFTS cell (Praying Mantis Kit, Harrick Scientific Corp.) fitted with zinc selenium (ZnSe)

windows. DRIFT spectra are recorded by a Nicolet 6700 FTIR spectrometer equipped with a mercury cadmium telluride (MCT) detector cooled with liquid nitrogen.

The temperature of the sample is measured using a thermocouple placed right below of the sample holder and is monitored/controlled with a Harrick temperature controller (Pleasantville, USA).

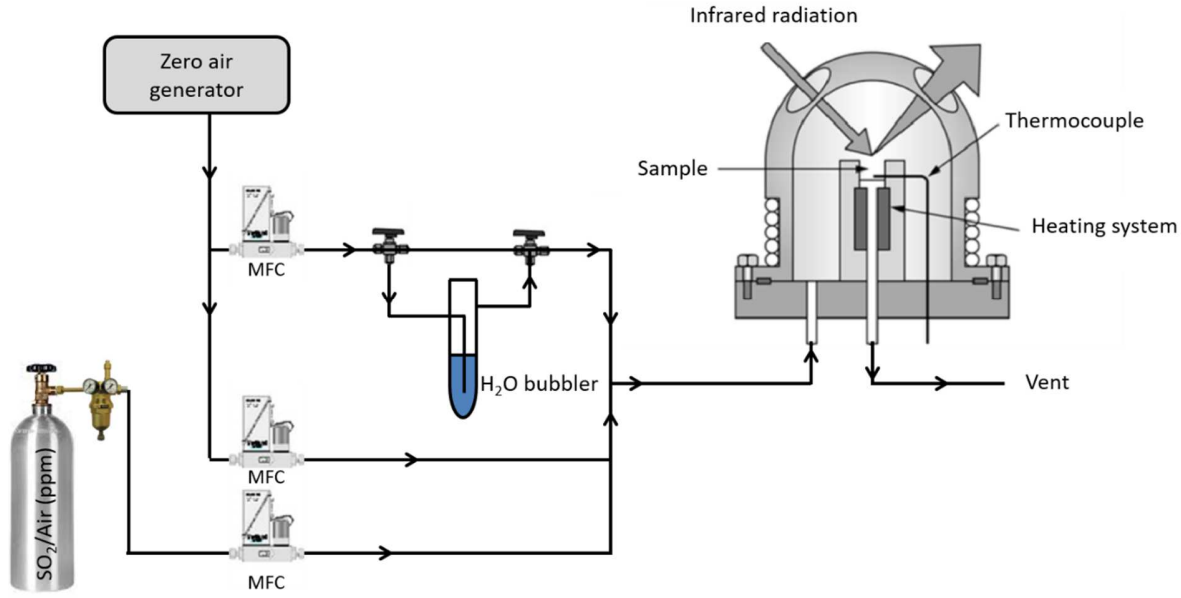

Figure 4: Scheme of the DRIFT experimental setup. MFC: Mass Flow Controllers are used to supply the optical cell with a defined mixing ratio of dry air, humid air, and SO_2.

At the beginning of the experiment the crucible sample holder inside the DRIFTS cell is filled with about 80-110 mg of v-dust. The cell is then tightly closed and the infrared beam is focused on the surface of the dust. The gas flowed through the DRIFTS cell is made up of different proportions of dry air, humid air and SO_2 gas. Prior to the introduction of the SO_2 gas volcanic samples are heated to 423 K for 1.5 hours to remove any pre-adsorbed species. Samples are then allowed to cool down to room temperature and are purged overnight with either dry or humid air depending on the experimental conditions in order to equilibrate the system. A background spectrum is recorded right before introduction of SO_2 gas. DRIFT spectra of the v-dust in the presence of SO_2 gas are recorded from 650 to 4000 cm^{-1} using Omnic software with 100 scans

per spectrum, a spectral resolution of 4 cm^{-1}, and a time resolution ranging from 3 minutes to 1 hour depending on the stage of the experiment. The formation and loss of surface species are observed as positive and negative absorption bands respectively. Thus, a typical experiment lasts about 4 days and consists of thermal pre-treatment (1.5 hr), system equilibration (16 hr), SO_2 adsorption phase (72 hr) and desorption upon flushing phase (6 hr). The SO_2 concentration in the mixed gas is 175 ppm. Note that this is over three orders of magnitude higher than the atmospherically relevant SO_2 concentration of ~75 ppb used in the flow-tube reactor experiments. Large difference in SO_2 concentrations used for flow tube versus DRIFTS experiments comes from different technical constrains. For instance, DRIFT spectroscopy is used for the in situ characterization of surface adsorbed species but is characterized by a relatively low sensitivity, depending on the gas-surface interactions. Likewise, the observation of the steady state in flow tubes, when the flowing gas is in ppm level, is not possible. In this work two different reactors serve two different purposes: flow tube is used to study kinetics by providing uptake coefficients under atmospherically relevant conditions while DRIFTS is used to study surface reaction mechanism. It is important to keep in mind that while the kinetics is changed by the concentration because the surface coverage is changed by the concentration, the reaction mechanism is not likely to be changed as a function of gas phase concentration. Thus, both techniques bring complimentary and valuable information.

2.2.3 Ion analysis

A reverse-phase HPLC method with indirect photometric detection for the simultaneous determination of sulfates and sulfites was used for quantification of sulfates and sulfites formed following experiments with DRIFTS. To prevent oxidation of sulfites to sulfates, 1.0 mL of 1% formalin in pure water is used as an extracting solvent as recommended by Michigami (Michigami and Ueda, 1994). After 20 min of mechanical shaking the extracted solution is passed through a 0.2 µm PTFE membrane and a filtered leaching solution is analyzed by Waters HPLC system. Chromatography equipment consists of Waters 2695 Series HPLC System equipped with 2487 UV/VIS Dual wavelength absorbance detector, (Waters Corporation, Milford, MA). Empower 2 Data Acquisition System for LC (Copyright 2005, Waters Corporation, Milford, MA) is used to analyze the data. Analysis is performed using Restek Ultra Column C18, 5 µm, Length

250 mm, I.D. 4.60 mm column dynamically coated with 1.0 mM cetylpyridinium chloride in 7% acetonitrile solution to produce a charged surface as recommended by Zuo et al. (Zuo and Chen, 2003) The HPLC instrument is operated isocratically at ambient temperature using Methanol-Potassium Hydrogen Phthalate Buffer 1.0 mM, adjusted to pH 6.5 with dilute potassium hydroxide (1:99, v/v) mobile phase and run at a flow rate of 1 mL/min for 15 min. The injection volume is 10 µL. Detector is set at 255 nm. All chemicals and solvents used for HPLC analysis are of analytical grade.

3. RESULTS AND DISCUSSION

3.1 Exploring SO_2 uptake on v-dust from the gas phase: flow tube study

3.1.1 First insight on SO_2 uptake on various natural v-dusts under ambient conditions

The uptake of atmospheric relevant concentration of SO_2 (i.e. ≈ 75 ppb) by the surface of five selected v-dusts under typical atmospheric conditions of ambient temperature, pressure and 30% *RH* was investigated using the flow tube reactor (Lasne et al., 2018). A typical uptake profile depicted in Figure 5 shows the $[SO_2]$ uptake of Mýrdalssandur dust in humid (*RH* = 30%) conditions. It is clearly observed from the profile that after the initial uptake of the gas upon exposure of the v-dust the system reaches a steady-state $[SO_2]$ that is distinct from the initial state $[SO_2]_0$, evidencing continuous consumption of the title molecule at least for the duration of the experiment. All the samples under investigation demonstrated both an initial uptake and a steady state uptake (similar to Figure 5). The latter is worth investigating as it suggests the ability of the v-dusts to exhibit a long-term effect on the equilibrium composition of the atmosphere. The steady state coefficients are in the order of 10^{-9} to 10^{-8} (Figure 6, Table 3). These values are much lower than the values obtained by Maters et al., who reported the initial uptakes of SO_2 on volcanic ash and glass powders at 10^{-3} to 10^{-2} range (Maters et al., 2017). Large difference in values is not surprising though for a number of reasons. First, the initial uptake describes an uptake on the fresh surface at the first instances of its interaction with gas, while the steady state uptake is an ongoing phenomenon reflecting the ability of the surface to adsorb gas continuously. Second, while determining initial uptakes geometric surface area was used by Maters et al. in order to calculate uptake coefficient (Maters et al., 2017), while specific surface area was used in this

study in order to account for all the surface accessible to the SO_2 molecules on longer time scales. Using geometric vs specific surface area gives an upper value for the uptake coefficient (Crowley et al., 2010). Finally, in the study of Maters et al. experiments were performed under dry conditions contrary to 30% *RH* used in this study. Moreover, in the adsorption/desorption experiments on the volcanic glasses performed by Schmauss and Keppler it was observed that the first layer of SO_2 molecules was adsorbed on the surface of volcanic glass irreversibly and could not be removed (Schmauss and Keppler, 2014).

Interestingly, the obtained results show somewhat contrasted behaviors from one sample to another. In the literature the differences in the uptake of SO_2 on solid material are commonly linked to the differences in elemental composition or minerology (Maters et al., 2017), (Maters et al., 2016), (Usher et al., 2002), (Zhang et al., 2006), (Harris et al., 2012). Using synthetic and natural silicate glasses as proxies for fresh unweathered volcanic ash is commonly done due to the fact that glass often represents a major component of v-dust. Besides, a thin layer of glass covering the crystalline components of ash surfaces was observed (Delmelle et al., 2018). Several studies indicated that sulfates are more likely to get adsorbed on the glass fraction of volcanic dust (Schmauss and Keppler, 2014), (Farges et al., 2009). While investigating trends in adsorption of SO_2 on glass, elemental composition is commonly investigated (Maters et al., 2017). This approach though ignores the crystalline phase of the volcanic dust. Maters et al. emphasized that the influence of crystallinity on the adsorption of SO_2 gas is not yet understood (Maters et al., 2017). On the other hand author working with natural mineral dust samples, such as desert dusts often approximate composition of dusts using simple mineral oxides and look for trends in adsorption in relationship with the mineral phase composition. In our study v-dusts differ significantly in their crystalline fraction. Volcanic samples used in this study contain from 20% (Hagavatn) to 80-90% (Mýrdalssandur, Maelifellssandur and Dyngjusandur) of amorphous material (Baratoux et al., 2011), (Moroni et al., 2018). The remaining part is crystalline. Eyjafjallajokull is also dominated by glass (Gislason et al., 2011). Plagioclase, pyroxene, and olivine are the mineral phases reported in all five samples, while magnetite was only found in Myrdalssandur and Maelifellsandur (Moroni et al., 2018), (Baratoux et al., 2011) (Gislason et al., 2011). A very small amount of crystalline silica was found in Eyjafjallajokull and none was reported for other samples (Gislason et al., 2011).

Since amorphous fraction dominates composition of v-dusts, an attempt to find trends in the uptake vs elemental composition was undertaken. Among the authors linking the differences in uptake coefficient to the elemental composition Maters et al. observed increase of the initial uptake of SO_2 on the surface of synthetic volcanic glasses with decrease of their silica (Si) content and increase of the sum of their sodium (Na), potassium (K), magnesium (Mg) and calcium (Ca) content (Maters et al., 2017). As for the natural volcanic samples the relationship was not as straightforward, even though a dependence of the initial uptake on the total surface content of the sum of Na, K, Mg and Ca was suggested (Maters et al., 2017). In our studies no clear correlation between the bulk elemental composition of a v-dust and its uptake of SO_2 was established. It can be due to the fact that the elemental concentration in the bulk sample may not represent the availability of the elements on the surface. Therefore, one might expect the information derived from elemental surface composition to be more accurate, yet care must be taken in interpreting such results. One should keep in mind that a given element when incorporated in glass versus crystalline mineral might behave differently. Farges et al. observed that crystalline quartz does not adsorb any sulfur species while amorphous silica does (Farges et al., 2009). The heterogeneous nature of the sample might further complicate finding the trends as elements forming different mineral phases will behave differently depending on the nature of mineral phase. For example, Fe is incorporated in both ilmenite ($FeTiO_3$) and fayalite (Fe_2SiO_4), yet the SO_2 uptake is significantly higher for the former mineral (Harris et al., 2012).

Earlier studies can be used to understand potential contribution of crystalline fraction of the volcanic ash to the uptake of SO_2. Both quartz (SiO_2) and magnetite (Fe_3O_4) can be found in volcanic ash. Comparison of the uptakes of SO_2 on individual mineral oxides, such as CaO, Al_2O_3, $CaCO_3$, Fe_3O_4 and Fe_2O_3 showed that the uptake of SO_2 depends on the nature of the mineral oxide with higher uptakes observed when SO_2 interacted with iron-containing compounds (Usher et al., 2002). These observations were further tested by Zhang et al. who compared reactivity of different oxides taking into consideration their specific area and placed them in the following order: Fe_2O_3>MgO>TiO_2>FeOOH>mixture>Al_2O_3>SiO_2 (Zhang et al., 2006). Both studies indicate that conversion of SO_2 per unit surface of Fe_2O_3 is the highest, suggesting that particles with the highest amount of iron might be the most reactive in reactions with SO_2. Furthermore, the reactivity of the mixture, that was obtained by mixing the different oxides based on their abundance in the continental crust, was measured to be twice its theoretical value, which

demonstrates its synergistic effect (Zhang et al., 2006). Even though most studies use simple mineral oxides and synthetic dust as a substitution for natural samples, such approach is problematic, as it undermines the importance of more complex mineralogy in the uptake of SO_2. While studying the uptake of SO_2 on Saharan dust Harris et al. distinguished ilmenite ($FeTiO_3$), rutile (TiO_2) and iron oxides (Fe_2O_3, Fe_3O_4, FeOOH) ($\gamma_{BET(mixture\ of\ ilmenite\ and\ rutile)}=3\times10^{-5}$) as major phases of dust responsible for uptake and oxidation of SO_2 (Harris et al., 2012). Uptake on feldspar minerals such as $KAlSi_3O_8$, $NaAlSi_3O_8$ or $CaAl_2Si_2O_8$ and quartz (SiO_2) was found to be slow ($\gamma_{BET(feldspar)}=9\times10^{-7}$, $\gamma_{(quartz\ with\ basic\ components)}=4\times10^{-8}$) (Harris et al., 2012). To identify the elements associated with adsorption of SO_2 by crystalline material Harris et al. analyzed individual Saharan dust grains that were relatively rich in S content after their exposure to SO_2 and studied their elemental profile using single-particle SEM–EDX analysis (Harris et al., 2012). Ti, Fe and Ca were identified as the most important reactive elements, while Na, Mg, Al, Si showed no relationship to oxidizing capacity of dust (Harris et al., 2012). While studying the uptake of SO_2 on v-dusts it would be informative to investigate the uptake of SO_2 on other complex mineral phases present in v-dust such as pyroxene, plagioclase, amphibole, biotite, and olivine even though higher uptakes of SO_2 are linked to the presence of minerals lacking silicates, such as ilmenite ($FeTiO_3$) and magnetite (Fe_3O_4) (Harris et al., 2012).

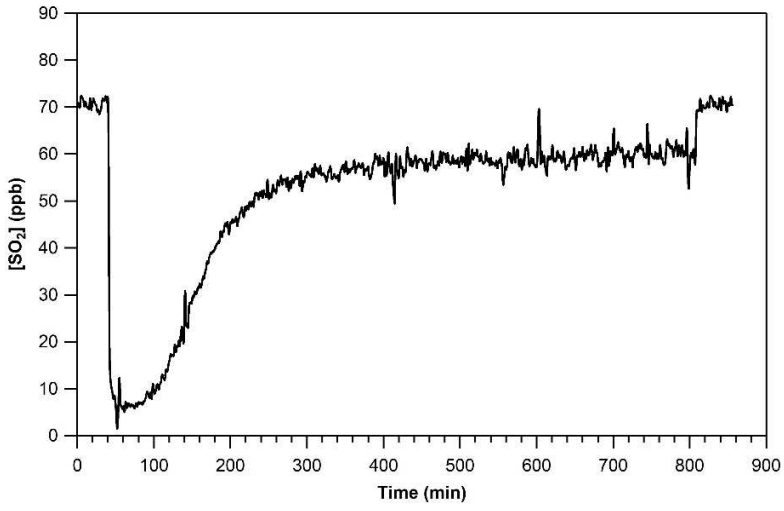

Figure 5: SO_2 concentration recorded by the analyzer during exposure of Mýrdalssandur v-dust at T = 296 K, RH = 30 %.

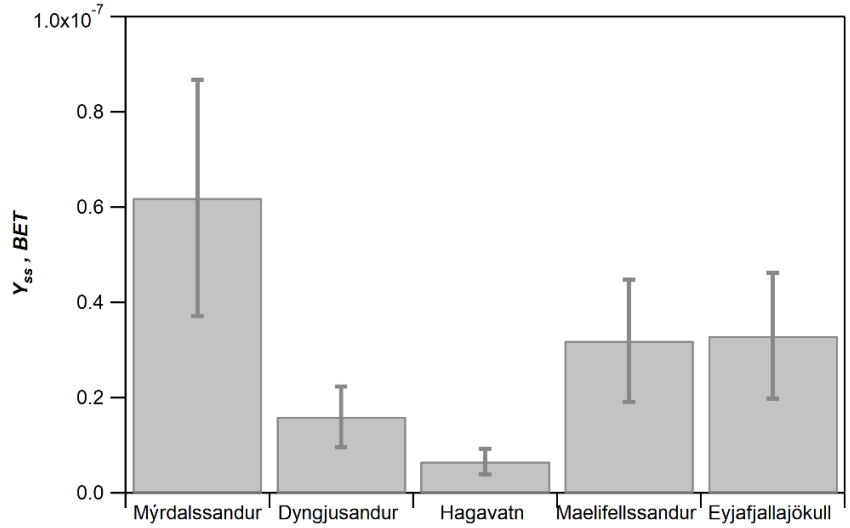

Figure 6: Steady-state uptake coefficients of the Icelandic v-dust samples at $[SO_2]_0 \approx 75$ ppb, RH = 30 %, T = 296 K, under dark conditions. The errors quoted reflects the total error for the steady state uptake coefficient determination.

Origin of the Icelandic v-dust	$\gamma_{SS,BET}$	N_s (molecules cm^{-2})
Mýrdalssandur	**$(6.2 \pm 2.5) \times 10^{-8}$**	**$(2.5 \pm 0.8) \times 10^{13}$**
Dyngjusandur	**$(1.6 \pm 0.6) \times 10^{-8}$**	**$(2.1 \pm 0.6) \times 10^{13}$**
Hagavatn	**$(6.6 \pm 2.6) \times 10^{-9}$**	**$(1.2 \pm 0.4) \times 10^{13}$**
Maelifellssandur	**$(3.2 \pm 1.3) \times 10^{-8}$**	**$(9.6 \pm 2.9) \times 10^{12}$**
Eyjafjallajökull	**$(3.3 \pm 1.3) \times 10^{-8}$**	**$(1.2 \pm 0.4) \times 10^{13}$**

Table 3: SO_2 steady-state uptake coefficients ($\gamma_{SS,BET}$) and transient initial number of molecules adsorbed (Ns) on the surface of v-dusts. Experimental conditions: $[SO_2]_0 \approx 75$ ppb, RH = 30 %, T = 296 K, under dark conditions.

The number of SO_2 (N_s) molecules removed during the transient initial uptake process per surface area was also investigated and was calculated to be in the order of 10^{13} molecules cm^{-2} (Table 3). These values are comparable to the values obtained by Maters et al., who reported the total uptake capacity of SO_2 on volcanic ash and glass powders under dry conditions at 10^{11} to 10^{13} range (Maters et al., 2017). As with initial uptakes, total uptake capacity of SO_2 on the surface of synthetic volcanic glasses increased with decrease of their Si content and increase of their total Na, K, Mg, Ca content (Maters et al., 2017). As for the natural volcanic ash samples the relationship was less clear and the dependence on total surface Na, K, Mg, Ca content was suggested (Maters et al., 2017). Furthermore, as displayed in Figure 7, the transient number of

556 molecules adsorbed N_s at the initial stage of the exposure, and the steady state uptake coefficients
557 do not follow the same trend. On one hand, Mýrdalssandur seems to adsorb the highest amount
558 of molecules and it has the highest uptake coefficient. On the other hand, Hagavatn that has the
559 smallest uptake coefficient adsorbs almost the same amount of molecules as Eyjafjallajökull and
560 more than Maelifellssandur even though the latter two have an uptake coefficient that is twice as
561 high as uptake coefficient of Hagavatn. The discrepancies between N_s and $\gamma_{ss,BET}$ suggest that the
562 surface is modified upon its initial exposure to SO_2. Indeed, one should keep in mind that
563 adsorption behavior of SO_2 on each volcanic dust was characterized by measuring the steady state
564 uptake coefficients after 12 hours of exposure, i.e. after long processing, while the number of
565 molecules taken up was measured after the first 5 hours of the interaction where a transient uptake
566 was observed at the initial stage of the experiment. Differences in the observed trends could
567 indicate that at the initial stage of the experiment the surface of the dusts is modified due to SO_2
568 uptake and the corresponding formation of sulfites and sulfates, and these modifications affect
569 the surface reactivity at longer time scale when the $\gamma_{ss,BET}$ values are determined. The
570 modifications could explain why no correlation was noticed between the $\gamma_{ss,BET}$ and N_s with the
571 elemental composition of the v-dusts. Finally, the discrepancies could be due to the fact that the
572 nature of the governing processes behind the initial fast uptake and thus the high amount of
573 molecules adsorbed in the initial stage and those dominating the steady state uptake are
574 fundamentally different (Huthwelker et al., 2006).

575

576

577

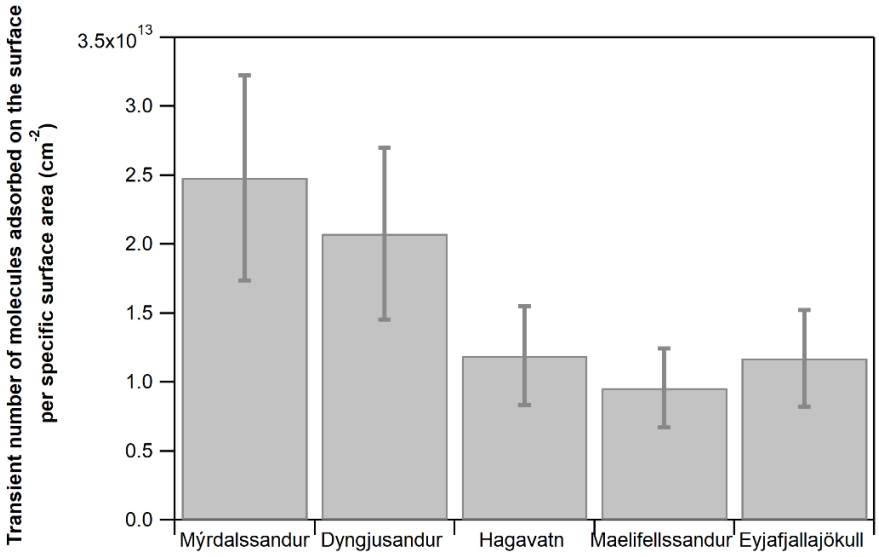

578

579

580 *Figure 7: Number of SO_2 molecules taken up on the surface of different v-dusts during the transient initial uptake process when*
581 *exposed to $[SO_2]_0 \approx 75$ ppb, T=296K, RH=30%, dark conditions. The errors quoted reflect the total error for the N_s*
582 *determinations.*

583 ### 3.1.2 The role of relative humidity on the uptake of SO_2 on v-dusts

584 Several studies have highlighted the role of *RH* on SO_2 uptake (Li et al., 2006), (Zhou et
585 al., 2014), (Huang et al., 2015). In order to investigate the role that *RH* plays in the steady state
586 uptake of SO_2 on v-dust samples the relationship was investigated for two contrasted samples
587 based on their steady-state uptakes – Mýrdalssandur and Hagavatn (Figure 8). For Mýrdalssandur
588 we observed that the steady state uptake coefficient of SO_2 at 30% of *RH* was significantly higher
589 than under dry conditions (i.e. $\gamma_{ss,\,BET}$ (30% *RH*) = 6.2×10^{-8} and $\gamma_{ss,\,BET}$ (dry) = 2.0×10^{-8}). For
590 the Hagavatn v-dust a similar trend was observed (i.e. $\gamma_{ss,\,BET}$ (30% *RH*) = 6.6×10^{-9} and $\gamma_{ss,\,BET}$
591 (dry) = 1.0×10^{-9}). The enhanced uptake trends observed in the presence of water indicate that
592 water plays an important role promoting the partitioning of SO_2 to the adsorbed phase. There
593 might be numerous reasons for the observed increased uptake of SO_2 in the presence of water
594 vapor. Adsorbed water molecules can (i) participate in the reactions as reactants, (ii) serve as a
595 medium for the reaction to take place or (iii) change the physical properties of the particle shifting
596 the equilibrium towards higher SO_2 uptake. Water molecules can also form water layers that can
597 help the product of the reaction to diffuse along the surface and thus promote the renewal, i.e. the
598 turnover, of surface sites (Shang et al., 2010). The intrinsic ability of metal oxides to adsorb water

molecules and form surface hydroxyls was linked to higher reactivity in the heterogeneous reaction with SO_2 (Zhang et al., 2006).

In the literature the analysis of the influence of *RH* on the uptake of SO_2 on natural mineral dusts shows complex trends. An influence of water vapor on the interaction of SO_2 with Saharah dust at 258 K showed no effect on initial uptake within statistical error (i.e. γ_{BET} (27% *RH*) = (6.0 ± 1.0) × 10^{-5} and γ_{BET} (dry) = (6.4 ± 0.7) × 10^{-5}) . Likewise, no dependency of the initial uptake coefficient on humidity was found for Adobe clay soil taken from Los Angeles area (Judeikis and Stewart, 1976). Alternatively, when Huang et al. subjected three authentic dusts to SO_2 at *RH* ranging from 0 to 90% an increase in uptake coefficient was observed for Tengger Desert dust (i.e. γ_{BET} (dry) ≈ 3.8 × 10^{-5} and γ_{BET} (90% *RH*) ≈ 5.5 × 10^{-5}) and for Arizona test dust (i.e. γ_{BET} (dry) ≈ 1.3 × 10^{-5} and γ_{BET} (90% *RH*) ≈ 2.76 × 10^{-5}), but a decrease was observed for Asian mineral dust (i.e. γ_{BET} (dry) ≈ 3.2 × 10^{-5} and γ_{BET} (90% *RH*) ≈ 1.9 × 10^{-5}) (Huang et al., 2015). The negative dependence of humidity on SO_2 uptake in the case of Asian mineral dust was explained by the presence of water-soluble inorganic coating, which made surface more acidic and inhibited uptake of SO_2(Huang et al., 2015). When the Asian mineral dust was washed and coating was removed, the uptake trend got reversed and showed positive correlation (i.e. γ_{BET} (dry) ≈ 0.85 × 10^{-5} and γ_{BET} (90% *RH*) ≈ 1.32 × 10^{-5})(Huang et al., 2015). Then again, while the samples from Inner Mongolian desert, characterized by high carbonate contents, demonstrated considerably increased uptakes at higher humidity (i.e. $\gamma_{ss, BET}$ (40% *RH*) = 1.0 × 10^{-6} and $\gamma_{ss, BET}$ (dry) = 1.7 × 10^{-7}), Xinjiang sierozem natural mineral dust showed only a modest increase in steady-state uptake (i.e. $\gamma_{ss, BET}$ (40% *RH*) ≈ 2.4 × 10^{-7} and $\gamma_{ss, BET}$ (dry) ≈ 2.2 × 10^{-7}) (Adams et al., 2005). The authors suggest that difference in the minerology could be responsible for the difference in the observed trends (Zhou et al., 2014). Higher carbonate component of the Inner Mongolian desert dust can promote the SO_2 uptake. Indeed, while investigating carbonate particles Zhang et al. observed that the value of the steady state uptake $\gamma_{ss, BET}$ drastically increases from $\gamma_{ss, BET}$ (1%) = 0.32× 10^{-8} to $\gamma_{ss, BET}$ (85% *RH*) = 13.9 × 10^{-8}), at 85% *RH* reaching 43 times its value at 1% (Zhang et al., 2018). In our study volcanic dusts, void of carbonates, cannot be directly compared to carbonate-rich samples, but the observed trend follows the one of Tengger Desert dust and Arizona test dust discussed earlier. More information about influence of humidity on the steady state uptake of SO_2 on the surface of volcanic glass and ash is necessary to obtain a more comprehensive picture.

While the increase in the SO_2 uptake with the increase of relative humidity is observed for a number of samples, it is not at all the case for the uptakes of other species, such as nonpolar volatile organic compounds (Romanias et al., 2016), hydrogen peroxide (H_2O_2) (Romanias et al., 2012) or ozone (O_3)(Lasne et al., 2018). In fact, the uptake coefficient can decrease with increased humidity, such as the case for the steady state uptake of O_3 on montmorillonite clay dust reflecting the tendency for the molecules in question and molecules of water to compete with each other for the sorptive sites on the clay surface (Lasne et al., 2018).

The observation of the steady state nature of the uptakes points out that there are important and maybe cyclic processes occurring on the surface of the v-dust. The gas phase monitoring limits us to the determination of kinetic parameters; in order to investigate the mechanism of the SO_2 uptake surface monitoring is necessary. Increased SO_2 uptake at higher *RH* suggests that humidity plays a particularly important role in the adsorption of SO_2 to the surface. To monitor the adsorbed phase, determine the functional groups that are involved in the adsorption of SO_2 and to further evaluate the role of water to the reaction system, a series of experiments were carried out employing DRIFT spectroscopy.

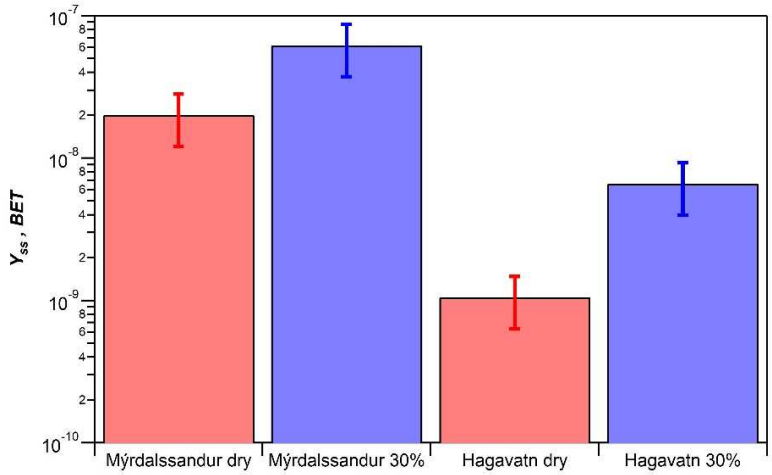

Figure 8: Steady-state uptake coefficients of the Mýrdalssandur and Hagavatn v-dust samples at RH = 30 % (blue bars) and RH=0% (red bars), $[SO_2]_0 \approx 75$ ppb, T = 296 K, under dark conditions. The errors quoted reflects the total error for the steady state uptake coefficient determination.

3.2 Exploring SO_2 uptake on v-dust from the adsorbed phase: DRIFTS study

While flow tube reactor monitors changes in the gas-phase concentration, DRIFTS focuses on changes on the solid phase. It is commonly used to study fine particles and powders, and can be used to investigate adsorption of molecules on solid surfaces. In this case spectra are collected as difference spectra with the unexposed solid as background. As the reaction proceeds, growing or decreasing peaks can be attributed to the species formed or consumed on the surface. Infrared spectroscopy based on light diffuse reflectance offers information about the vibrational modes associated with stretching, bending, and rocking motions of the adsorbed molecules. However, in order to monitor these vibrations the sample has to have high enough reflectance to insure an adequate signal in response to changes in the adsorbed phase, and the surface concentration needs to be high enough due to the low sensitivity of the technique. If the sample is highly absorbent, which is the case of v-dust samples, it is usually diluted in a non-absorbent matrix, such as KBr. In our case, however, this type of matrix could not be used because of the interactions of KBr with SO_2 and thus the use of pure v-dust was required. The background obtained for each v-dust under dry conditions showed that all of them absorb light strongly and, as a result, a weak IR signal was recorded in response to changes in the adsorbed phase. To study the adsorption of SO_2 on v-dust, backgrounds of five samples were taken to choose the least absorbent varieties. In comparison with other v-dusts the background for Hagavatn and Eyjafjallajökull shows higher reflectance in the area from 800 to 1350 cm^{-1} where sulfite and sulfate species usually absorb. Because of its higher reflectance and higher specific surface area, Hagavatn v-dust was selected as the most appropriate sample for DRIFTS experiments. Besides, results obtained from the flow tube studies showed similar trends in SO_2 adsorption by the v-dusts based on gas-phase monitoring of SO_2, i.e. rapid consumption of SO_2 gas at the initial stage of surface exposure followed by a steady state removal of the probe molecule. Therefore, it appeared justified to choose one dust as a representative sample to study the mechanism of product formation on the surface of aerosols. Aiming to further investigate the observations from the flow tube study and to further assess the role of humidity on the reaction mechanism, the DRIFTS experiments were performed under dry conditions and 30% *RH* using Hagavatn as a sample material.

3.2.1 Typical DRIFT spectra of SO_2 interaction on v-dust

Figure 9 and Figure 10 show DRIFT spectra of Hagavatn v-dust at increasing SO_2 exposure time intervals at room temperature under 0% and 30% *RH* respectively. Table 4 introduces the assignment of peaks of different adsorbed sulfur-containing species as well as water and hydroxyl groups on the surface of v-dust investigated and different metal oxides found in the literature.

In Particular, the negative and positive absorption peaks in the area from 4000 to 3500 cm^{-1} correspond to the free OH groups that are naturally present on the surface of v-dust (Hair, 1975). These groups are attached to the surface atoms, such as Si for example, and can be either completely isolated or hydrogen-bonded to each other (Hair, 1975). Adsorption of molecules containing a lone-pair of electrons is often associated with isolated surface OH groups, while neighboring hydrogen-bonded surface OH groups are involved in the adsorption of water (Hair, 1975), (Nanayakkara et al., 2012). The exact assignment of each individual peak is not possible due to the complex response reflecting slightly different vibrational energies of OH groups bonded to different minerals composing the v-dust. A peak from 3500 to 2600 cm^{-1} and another peak from 1800 to 1400 cm^{-1} centered at 1620 cm^{-1} (not displayed) are attributed to vibration modes in molecular water (Hair, 1975).

A weak broad peak from 2600 to 2400 cm^{-1}, visible under humid conditions, could be assigned to the S-H stretch vibration of the HSO_3^- bisulfite species that is only found in the literature as a theoretical value calculated by Zhang et al. for aqueous solution and reported to be in the range of 2620 to 2450 cm^{-1} (Zhang and Ewing, 2002). This peak is not visible under dry condition. Sulfur-containing products appear in the area from 1385 to 700 cm^{-1} under humid conditions and from 1367 to 716 cm^{-1} under dry conditions. Spectra under humid conditions are better resolved and several peaks can be distinguished: 3040, 2500, 1364, 1220, 1135, 930 and 872 cm^{-1}. Peaks under dry conditions are much noisier, nevertheless the following peaks are observed: 3242, 1340, 1230 and 1150 cm^{-1}. A double peak centered at 1364 cm^{-1} under humid conditions and at 1340 cm^{-1} under dry conditions appears rapidly upon exposure of the surface to SO_2 gas and disappears right away from the spectra after ceasing the SO_2 flow. It was therefore assigned to the weakly, reversibly physisorbed SO_2 species. The peak corresponds well to the literature values for SO_2 adsorption under dry conditions on the surfaces of aluminum, magnesium or titanium oxides identified in the previous studies at 1330 cm^{-1} and its gas-phase

711 value of 1362 cm^{-1} (Nanayakkara et al., 2012), (Goodman et al., 2001). Another band appears
712 rapidly upon exposure of SO_2 to the surface between 1053 and 700 cm^{-1} under humid conditions.
713 A corresponding band between 975 and 716 cm^{-1} under dry conditions takes more time to develop
714 and is hard to interpret since its intensity is almost at the limit of detection of the DRIFTS
715 instrument. The assignment of this band is based on the previous assignments of SO_2 adsorption
716 on the surface of different metal oxides found in the literature and corresponds to the stretching
717 motion of sulfite and bisulfite species that are bonded to the surface in a monodentate or bidentate
718 mode. Different coordination environments as well as heterogeneous nature of v-dust contribute
719 to the broadening of the band (Usher et al., 2002). In particular, Goodman et al (Goodman et al.,
720 2001)., Usher et al. (Usher et al., 2002) and Zhang et al. (Zhang et al., 2006) assigned the band
721 between 1100 to 850 cm^{-1} to adsorbed sulfite and bisulfite on α-Al_2O_3 and MgO. Li et al. (Li et
722 al., 2006) and Wu et al. (Wu et al., 2011) assigned a 1000-900 cm^{-1} band on $CaCO_3$ to a stretching
723 vibration of sulfite. A peak from 1200 to 800 cm^{-1} on TiO_2 was assigned to sulfite and bisulfite
724 species by Nanayakkara et al. (Nanayakkara et al., 2012). On hematite particles Wang et al.
725 assigned to sulfites a peak between 950 and 800 cm^{-1} under dry conditions and a series of peaks
726 from 1050 to 900 cm^{-1} under humid conditions (Wang et al., 2018b). Finally, a band from 1320
727 to 975 cm^{-1} with features at 1230 and 1150 cm^{-1} in dry conditions and from 1302 to 1055 cm^{-1}
728 with features at 1220 and 1135 cm^{-1} under humid conditions was attributed to sulfate and bisulfate
729 species. The assignment agrees well with the results published previously, where
730 sulfates/bisulfates were found around 1300-1100 cm^{-1} on α-Al_2O_3 and MgO (Usher et al., 2002),
731 (Zhang et al., 2006); between 1240 and 1012 cm^{-1} on $CaCO_3$ with features at 1198, 1127, and
732 1090 cm^{-1}(Wu et al., 2011), (Li et al., 2006). Sulfates were reported between 1300 and 1100 cm^{-1}
733 on TiO_2 (Nanayakkara et al., 2012), (Shang et al., 2010); and at 1220 cm^{-1} on Fe_2O_3 (Wang et
734 al., 2018b). Just as sulfites, sulfates can be bonded to the surface in bidentate or monodentate
735 modes (Jiang et al., 2010). A peak centered at 1220 cm^{-1} under humid conditions and at 1230 cm^{-1}
736 under dry conditions could be attributed to the formation of bisulfate species (Wang et al.,
737 2018a). The process of sulfate/sulfite formation is explained later in the reaction mechanism
738 section.

Molecular species (wavenumbers are expressed in cm^{-1})	V-dust (this work)	Si_2O_3	Al_2O_3	MgO	TiO_2	$CaCO_3$	Fe_2O_3	Theoretical calculations
SH stretch of HSO_3^-	2600-2400	2600-2400 (Hair, 1975)						2620 to 2450 (Zhang and Ewing, 2002)
SO_2	1364, 1340		1330, 1149 (Goodman et al., 2001)	1330, 1149 (Goodman et al., 2001)	1139, 1325 (Nanayakkara et al., 2012)		1400 (Nanayakkara et al., 2012)	
HSO_3^-/SO_3^{2-}	1053-700 975-716		1200-900 (Goodman et al., 2001) 1100-850 (Zhang et al., 2006)		1200-800 (Nanayakkara et al., 2012) 1080 (Shang et al., 2010)		Dry: 950-800 Humid: 1050-900 (Wang et al., 2018b)	
SO_3^{2-}				1125-800 (Goodman et al., 2001)	Monodentate: 1033, 971, 923 (Nanayakkara et al., 2012) Bidentate: 1006, 886(Nanayakkara et al., 2012)	1000-900 (Li et al., 2006) 1000-885 (Wu et al., 2011)	Dry:891 (Wang et al., 2018b) Humid: 981 (Wang et al., 2018b)	
HSO_3^-					1077 (Nanayakkara et al., 2012)			1054, 1154, 1219 (Zhang and Ewing, 2002)
HSO_4^-/SO_4^{2-}	1320-975 1302-1055		1245, 1170 (Usher et al., 2002)	1150, 1050 (Usher et al., 2002)		1240-1012 (Wu et al., 2011)		
HSO_4^-	1220, 1230						1219 (Wang et al., 2018a)	
SO_4^-			1300-1100(Zhang et al., 2006)	1300-1100 (Zhang et al., 2006)	1361, 1297, 1172, 1116, 1050, 1000 (Nanayakkara et al., 2012) 1300-1100 (Shang et al., 2010)	1130 (Li et al., 2006)	Dry: 1339-1014 Humid: 1208-1222(Wang et al., 2018b)	
free OH groups	4000-3500	4000-3500 (Hair, 1975)	3748, 3707 (Goodman et al., 2001)		3800-3600 (Nanayakkara et al., 2012) 1666, 3628 (Shang et al., 2010)		3704 (Wang et al., 2018b)	
OH groups of acids							3447, 3548 (Wang et al., 2018b)	3622 (Zhang and Ewing, 2002)
molecular water	3500-2600 1400-1800	3450, 1630 (Hair, 1975)	3524, 3296 (Goodman et al., 2001)		3160, 1654 (Shang et al., 2010)		3208, 1642 (Wang et al., 2018b)	

Table 4: Vibrational wavenumbers (cm^{-1}) of sulfur-containing species adsorbed on v-dust and metal oxides.

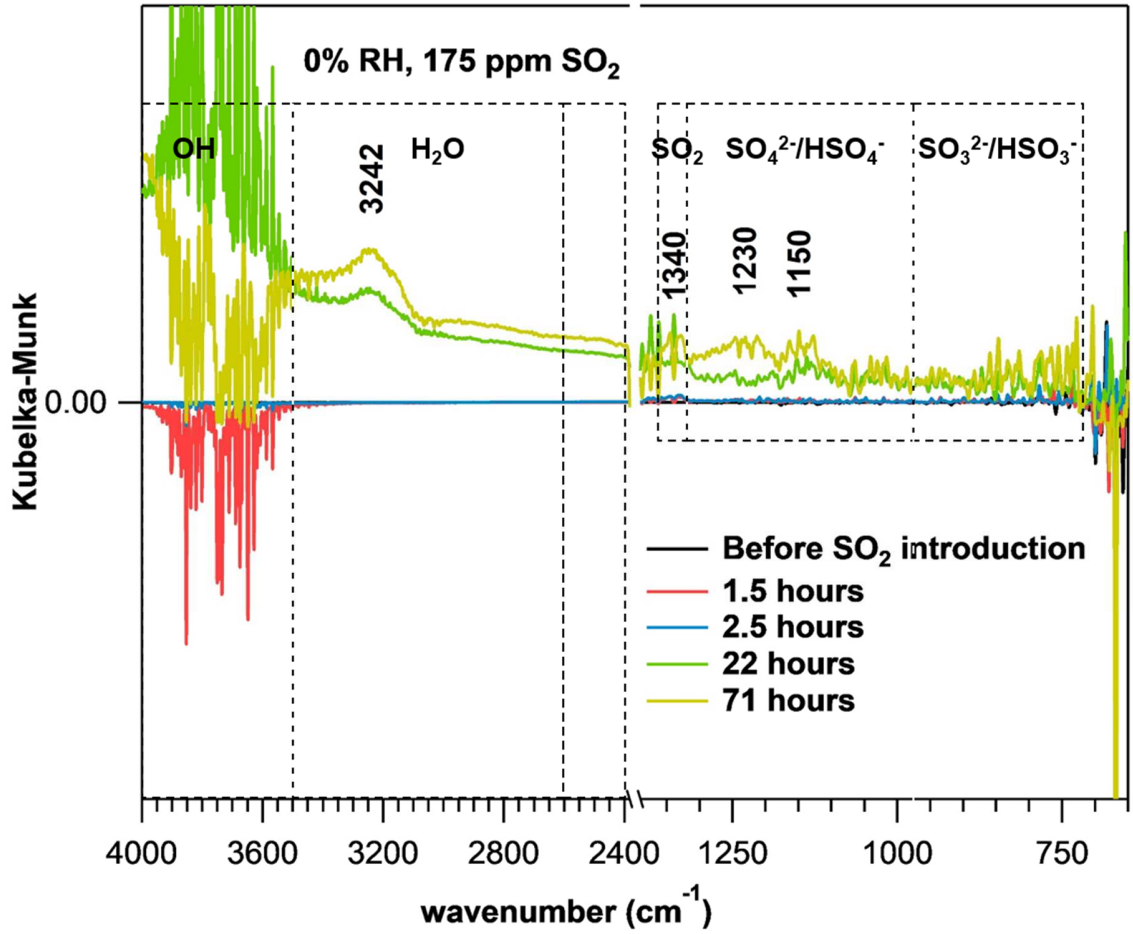

Figure 9: DRIFTS spectra of SO_2 uptake by Hagavatn v-dust at 0% RH and 296 K depicting evolution of bands for free surface OH groups (4000-3500 cm^{-1}), adsorbed water (3500-2600 cm^{-1}), physisorbed SO_2 (1385-1320 cm^{-1}), sulfates/bisulfates (1320-975 cm^{-1}), sulfites/bisulfites (975-716 cm^{-1}) as a function of time: black line – before introduction of SO_2, red line- after 1.5 h of exposure to SO_2, blue line- after 2.5 h of exposure to SO_2, green line- after 22 h of exposure to SO_2, yellow line- after 71 h of exposure to SO_2.

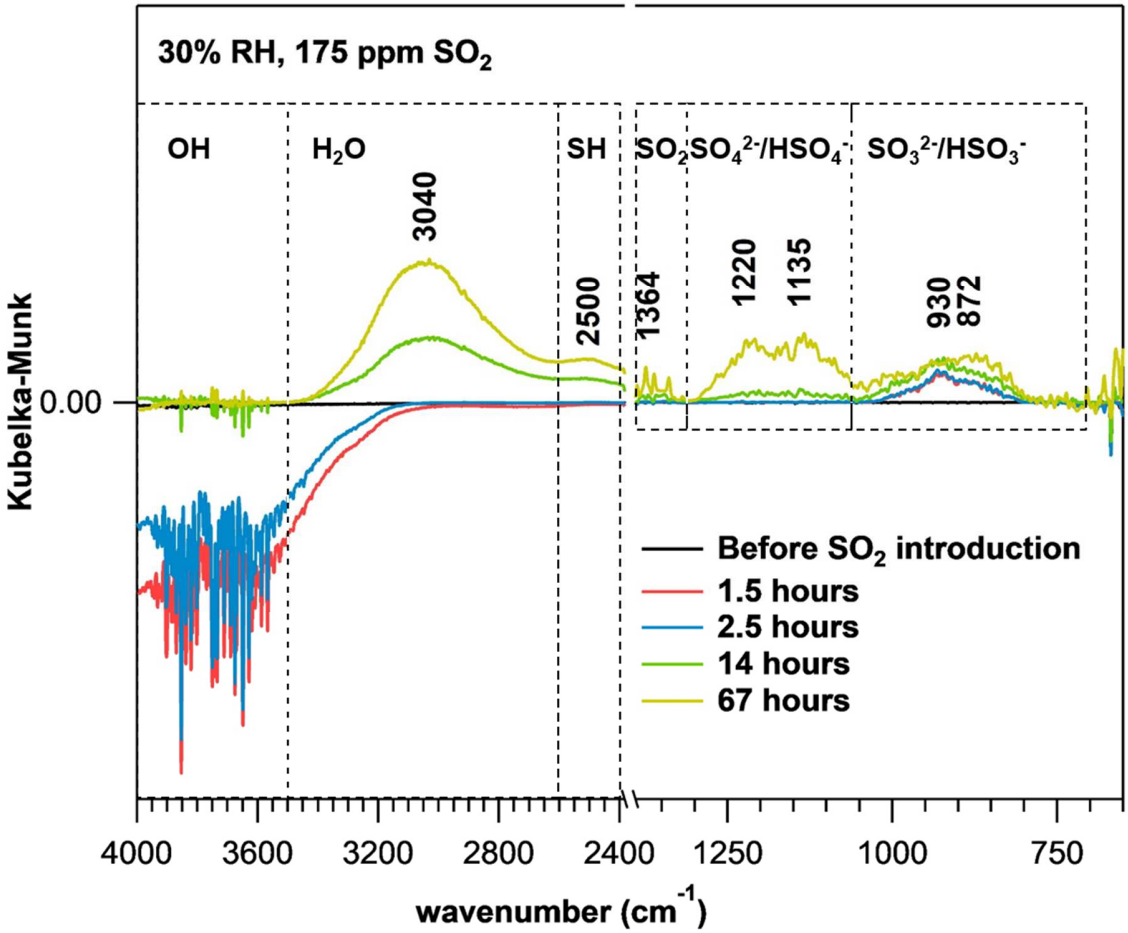

Figure 10: DRIFTS spectra of SO_2 uptake on Hagavatn v-dust at 30% RH and 296 K depicting evolution of bands for free surface OH groups (4000-3500 cm^{-1}), adsorbed water (3500-2600 cm^{-1}), SH groups (2600-2400 cm^{-1}), physisorbed SO_2 (1367-1320), sulfates/bisulfates (1302-1050 cm^{-1}), sulfites/bisulfites (1053-700 cm^{-1}) as a function of time: black line – before introduction of SO_2, red line- after 1.5 h of exposure to SO_2, blue line- after 2.5 h of exposure to SO_2, green line- after 22 h of exposure to SO_2, yellow line- after 71 h of exposure to SO_2.

3.2.2 Surface reaction mechanism.

Changes in the DRIFT spectra of the surface of Hagavatn v-dust are clearly seen upon introduction of SO_2 (Figure 9 and 10). In comparison with the studies of the interaction of SO_2 with pure metal oxides reported earlier by different researchers, it is evident that the peaks for sulfur-containing species appear much slower, most probably due to low sensitivity when dealing with dark v-dusts where the reflectance of the infrared light is limited (Zhang et al., 2006), (Usher et al., 2002), (Goodman et al., 2001), (Li et al., 2006), (Wu et al., 2011), (Nanayakkara et al., 2012), (Shang et al., 2010), (Wang et al., 2018b). The time evolution of five peaks corresponding

to different species, such as free OH groups, molecular water, physisorbed SO_2, sulfites/bisulfites and sulfates/bisulfates is followed.

3.2.2.1 Dry conditions

From our flow tube experiments presented earlier it is apparent that SO_2 gas is massively lost from the gas phase upon its exposure to the v-dust surface. Interestingly, the first peaks that appear in the DRIFT spectra after introduction of SO_2 gas are positive peaks for physisorbed SO_2 gas and negative peaks for free OH groups (Figure 9). Note that although the sample has been thermally pretreated and the experiment is performed under dry conditions, surface OH groups are present on the surface of the sample. The complete dehydroxylation of the surface would have required stronger thermal pretreatment. The loss of surface free OH groups reaches its local minimum at around 1.5 hr exposure to SO_2 before returning to its initial pre-exposed level where it starts fluctuating around zero. The peak for SO_2 gas is stable, but hard to integrate due to its small size and overlap with a much more pronounced peak for bulk water. Bulk water peak is highly unstable. The disappearance of free OH groups and appearance of physisorbed SO_2 suggest that in the first instants of the reaction, SO_2 gas gets weakly bonded to hydroxyl groups of the surface as first proposed by Datta et al. and later proved by theoretical calculations by Lo et al. for γ-alumina (Datta et al., 1985), (Lo et al., 2010). Maters et al. suggested that due to the weakly acidic nature of SO_2 gas its uptake is likely to happen on strongly basic sites affiliated with alkaline and alkaline earth metals on the surface of the volcanic glass (-K-OH, -Mg-OH, -Ca-OH, Mg-OH)(Maters et al., 2017). At the same time it is also possible for the SO_2 gas to get adsorbed on metallic Lewis acid sites of mineral phase as proposed by Wang et al. (Wang et al., 2018a). Hence, the first interaction of SO_2 gas with the surface under dry conditions is its distribution on different sites of the v-dust leading to a reversible physisorption of SO_2, as indicated by subscript *(ads)* (Reaction 1). Throughout the manuscript the chemisorbed species or chemical groups that form a chemical bond with the surface are indicated as *(surface)*.

Reaction 1

$$\mathbf{SO_{2(g)} \leftrightarrow SO_{2(ads)}}$$

Physisorbed SO_2 can then participate in reactions leading to chemisorbed species. Sulfites and sulfates, under dry conditions first appear after several hours of exposure probably due to the

low sensitivity of our DRIFT setup, as abovementioned. Sulfites can be formed on the lattice oxygen sites that can be viewed as Lewis basic sites (Wang et al., 2018a) as in Reaction 2.

Reaction 2

$$SO_{2(ads)} + O^{2-}{}_{(lattice)} \rightarrow SO_3^{2-}{}_{(surface)}$$

Alternatively, sulfites can be formed in the presence of hydroxyl groups as SO_2 can react with either one hydroxyl group to form bisulfite (Reaction 3) or two neighboring hydroxyl groups to form sulfite and water (Reaction 4) (Wang et al., 2018a). Surface hydroxyl groups themselves can be bonded to a single metal atom or bridge two, creating different environments for interactions with SO_2 (Ullerstam et al., 2002).

Reaction 3

$$SO_{2(ads)} + OH^-{}_{(surface)} \rightarrow HSO_3^-{}_{(surface)}$$

Reaction 4

$$SO_{2(ads)} + 2OH^-{}_{(surface)} \rightarrow SO_3^{2-}{}_{(surface)} + H_2O$$

Chemisorption of SO_2 gas on oxide anions (O^{2-}) and hydroxyl groups of volcanic ash and glass leading to the formation of sulfites and bisulfites was suggested earlier by Maters et al. and detection of sulfites in the leachates confirmed the conversion (Maters et al., 2017).

From Figure 11 that shows time evolutions of sulfites and sulfates, it can be observed that, under dry conditions, sulfites (SO_3^{2-}) get completely stabilized after 22 hours of exposure, but sulfates (SO_4^{2-}) keep growing linearly, suggesting that sulfites are the intermediate species in the oxidation of SO_2 to sulfates. Oxidation of sulfites to sulfates on the surface of volcanic glass was observed by Farges et al. (Farges et al., 2009). Sulfites can be oxidized to sulfates via several pathways. Active oxygen derived from molecular oxygen adsorbed on the active sites (Reaction 7) can oxidize sulfites to sulfates and bisulfites to bisulfates as in Reaction 5 and Reaction 6 (Wang et al., 2018a).

Reaction 5

$$SO_3^{2-}{}_{(surface)} + O^-{}_{(ads)} \rightarrow SO_4^{2-}{}_{(surface)} + e^-$$

Reaction 6

$$HSO_3^-{}_{(surface)} + O^-{}_{(ads)} \rightarrow HSO_4^-{}_{(surface)} + e^-$$

Contrary to our observations and to results reported by Shang et al. (Shang et al., 2010), who also noticed a stable rate of sulfate production on the surface of titanium dioxide particles in the presence of oxygen, Usher et al. (Usher et al., 2002) noted complete saturation of mineral oxide surfaces with SO_2 gas and observed no sulfate formation even upon exposure of SO_2-treated surface to air and oxygen. It could be due to the fact that the minerals under investigation were not able to convert molecular oxygen into active oxygen under the specific experimental conditions of these measurements.

Reaction 7

$$O_{(vacancy)} + e^- + O_2 \rightarrow O_2^-{}_{(ads)}$$

$$O_2^-{}_{(ads)} + e^- \rightarrow 2O^-{}_{(ads)}$$

where e^- is a conductive electron trapped in the vacant oxygen site on the surface of some oxides that are prone to having defect sites, such as on the surface of Fe_2O_3, for example (Wang et al., 2018b), (Baltrusaitis et al., 2007). Noticeably, reaction proceeds in the absence of light (Baltrusaitis et al., 2007). Reaction 7 was reported to enable the conversion of sulfites to sulfates on the surface of mineral phase, but a similar process can be expected to happen on the amorphous fraction of the volcanic ash due to the high defect population on silicate glasses (A Leed and Pantano, 2003), (Farges et al., 2009) .

Additionally, certain metal centers that can be readily reduced, such as Fe^{3+} to Fe^{2+}, contribute to the formation of sulfates from bisulfites as per Reaction 8 (Wang et al., 2018a).

Reaction 8

$$HSO_3^-{}_{(surface)} + OH^-{}_{(surface)} \xrightarrow{Fe^{3+} \rightarrow Fe^{2+}} SO_4^{2-}{}_{(surface)} + 2H^+ + 2e^-$$

Finally, bisulfates can be oxidized to sulfates by hydroxyl groups as per Reaction 9 (Wang et al., 2018a).

Reaction 9

$$HSO_4^-{}_{(surface)} + OH^-{}_{(surface)} \rightarrow SO_4^{2-}{}_{(surface)} + H_2O$$

On ceasing the gas flow and flushing the system for 6 hours, the peak for sulfites decreases due to its oxidation as per Reaction 5, Reaction 6 and Reaction 8, while the peak for sulfates increases for a couple of hours before getting stable, at the same time slightly changing its shape. The peak centered at 1230 cm^{-1} gets smaller in comparison with the peak at 1135 cm^{-1} suggesting indeed further conversion of bisulfates to sulfates. A decrease in sulfite peak with simultaneous increase in the sulfate peak upon cutting off SO_2 supply and addition of O_3 was observed by Li et al. (Li et al., 2006). Thus, sulfates appear to be the final product of oxidation of SO_2 gas and they keep being formed on the surface as long as there are sulfites available for oxidation. Sulfates were also reported as a final irreversible product of the interaction of SO_2 gas with volcanic glass by Farges et al. and by Maters et al. (Farges et al., 2009), (Maters et al., 2017).

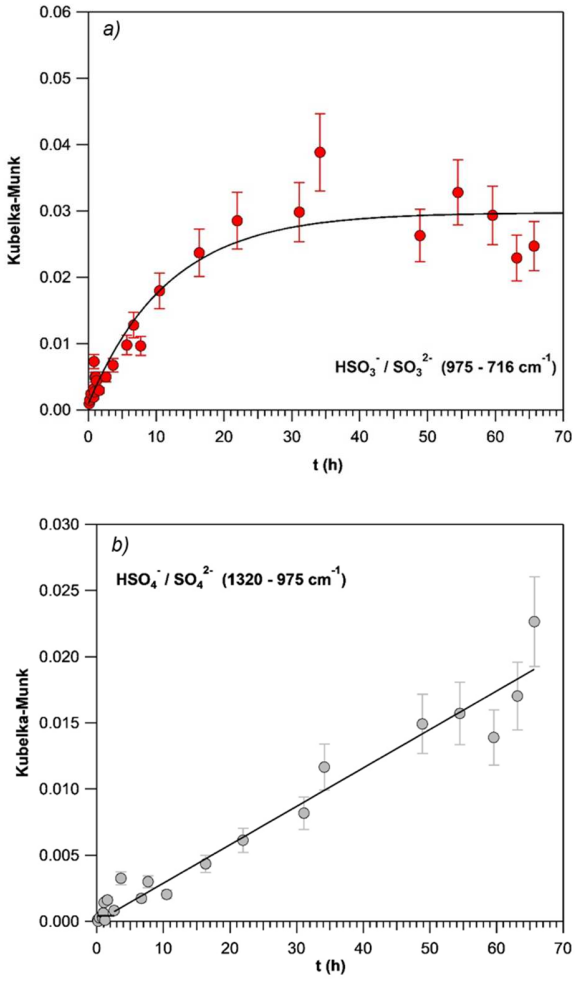

Figure 11: Integrated absorbance for (a) sulfites/bisulfites, (b) sulfates/bisulfates as a function of time under 0% RH and 296K. Upper graph: sulfites/bisulfites are stabilized after 22 hours of exposure. The solid line is an exponential fitting of experimental results to better display the observed trends. Lower graph: A linear growth of sulfates/bisulfates with time is noticed; note that

the peak is stable for the first couple of hours and then keeps increasing in a linear fashion. The solid line is the linear fit of experimental results.

3.2.2.2 Humid conditions

After exposure of v-dust to SO_2 gas under humid conditions the following changes are observed in the analysis of DRIFT spectra as seen in Figure 10 and Figure 12. At the very beginning of the experiment, the free OH groups get consumed and reach a minimum after 1.5 hours exposure to SO_2, at the same time sulfites form rapidly and at an almost linear rate. The peak for physisorbed SO_2 increases much slower and the peak remains small for the duration of the experiment. The initial time period corresponds well with the reaction mechanism proposed by Wang et al. in Reaction 3 and Reaction 4 both of which require consumption of free OH groups to produce sulfites and bisulfites. From 1.5 to 2.5 hours consumption of OH groups slows down and finally reaches a stable level. It is important to stress out that, when working under humid conditions, surface OH groups are continuously regenerated. The mechanism for metal oxide surface hydroxylation proposed by Tamura et al. assumes that an exposed oxygen center of the metal oxide lattice acts as Lewis base with water to form a surface terminal hydroxyl group and a hydroxide ion as shown in Reaction 10 (Tamura et al., 2001). In other words, a surface oxide ion gets neutralized by water to become $OH^-_{(surface)}$, while water itself loses a proton to become hydroxide ion $OH^-_{(ads)}$.

Reaction 10

$$\mathbf{O^{2-}_{(lattice)} + H_2O \rightarrow OH^-_{(surface)} + OH^-_{(ads)}}$$

Sulfates are first observed in the DRIFT spectra at 2.5 hours exposure to SO_2. Sulfates can be formed by three different pathways shown in Reaction 5, Reaction 6, and Reaction 8 (Wang et al., 2018a). Unlike sulfites, the peak for sulfates keeps growing linearly with time once again suggesting that sulfate is the final product of SO_2 oxidation and that the surface does not get saturated within the duration of the experiment. A peak for molecular water is hard to evaluate at 30% *RH* as water is being constantly supplied in large excess. Initially, the peak for water seems to decrease, which could be due to the competition with SO_2 gas molecules for active sites on the surface (Figure 10). At 14 hours the water peak stabilizes at a positive value, indicating that the surface is now storing more H_2O molecules than before introduction of SO_2 gas (Figure 10). Formation of sulfite and sulfate species could have changed equilibrium for adsorption of water on the dust surface (*e.g.* due to chemical changes of the mineral structure that increase the

hygroscopicity of the samples). Particularly, it was argued that adsorption of bidentate sulfate on the surface of Fe-Mn/TiO_2 catalyst increases the Lewis acid character of the metal ion to which it is attached, thus potentially favoring the adsorption of water on the metal center (Jiang et al., 2010). Finally, when the flow of SO_2 is stopped, the peak for sulfite gradually decreases while the peak for sulfate increases for a couple of hours, stabilizes and stays in the spectra for at least six hours. Like under dry conditions the peak for bisulfates/sulfates changes its shape by decreasing the peak associated with bisulfates (at 1220 cm^{-1}) suggesting its conversion to sulfates.

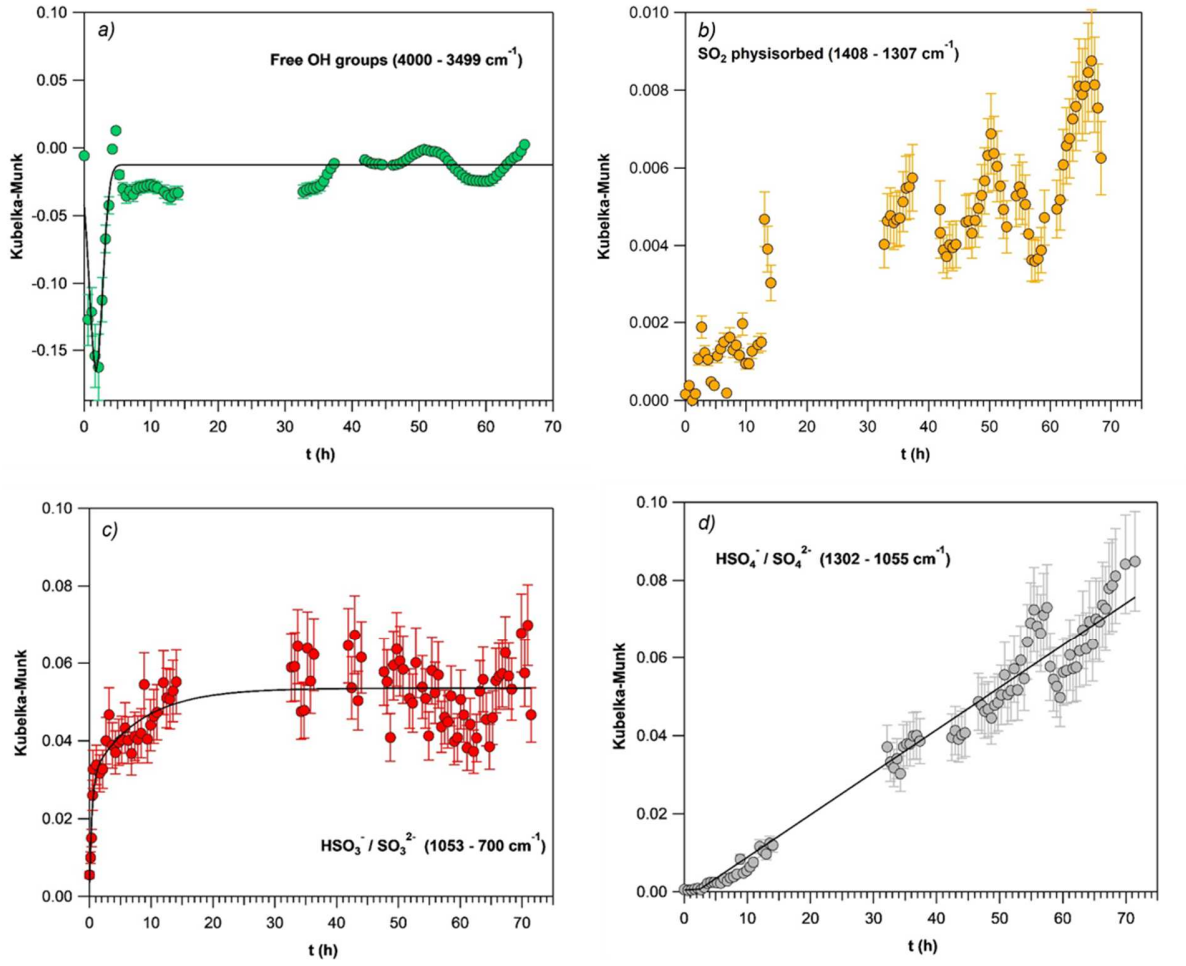

Figure 12: Integrated absorbance for (a) free hydroxyl groups, (b) physisorbed SO_2, (c) sulfites/bisulfites, (d) sulfates/bisulfates as a function of time under 30% RH and 296 K. The free OH groups get consumed very fast at the beginning of the experiment and reach a minimum at 1.5 hours, then the consumption of OH groups decreases and reaches a stable level at 2.5 hr. The solid line is an empirical fitting of experimental results to better display the observed trends. The peak for physisorbed SO_2 is quite nosiy but increases slowly and remains weak for the duration of the experiment. The solid line is an empirical fitting of experimental data points. Sulfites/bisulfites grow rapidly and almost linearly for the first 1.5 hr and then stabilize. The solid line is an exponential fitting of experimental results to better display the observed trends. The peak for sulfates/bisulfates is stable at low values for the first 2.5 hr and then increases in the linear fashion. The solid line is the linear fit of experimental results.

3.2.2.3 Comparison between dry and humid conditions

Although DRIFTS is a semi-quantitative technique, it is feasible to compare the results obtained under dry and humid conditions. Thus, in comparison with the reaction under dry conditions the reaction under humid conditions is much more pronounced, resulting in both faster reaction rates and higher integration values obtained for all sulfur containing species involved. This observation is in line with the results obtained from the flow tube experiments, where significantly higher steady state uptakes were determined for SO_2 under humid compared to dry conditions. Faster sulfite formation is most likely related to the dramatic increase in the amount of hydroxyl groups covering the surface under humid conditions, driving the sulfite and bisulfite formation through Reaction 3 and Reaction 4. Indeed, under humid conditions the amount of hydroxyl groups lost in the first minutes is much larger than under dry conditions, thus adsorbed SO_2 molecules convert rapidly to form sulfites (Figure 9 and Figure 10). Huang et al. reported that the rate of sulfate formation on the surface of Arizona test dust increased with *RH* and reached its maximum at 70% *RH* (Huang et al., 2015). Importance of surface OH groups in the heterogeneous oxidation of SO_2 gas was discussed by Zhang et al. who compared basic, neutral and acidic Al_2O_3 in their ability to oxidize SO_2 and noted that basic Al_2O_3 was much more efficient due to its higher concentration of hydroxyl groups on the surface (Zhang et al., 2006). It was also suggested that reactivity of different oxides to SO_2 uptake could be predicted by evaluating their intrinsic ability to form surface hydroxyl groups. Thus, metal oxides that have empty or half-empty d atomic orbitals, such as Al_2O_3, easily adsorb molecular oxygen and gaseous water and show excellent performance in the reactions with SO_2 while metal with full d orbitals, such as MnO_2, show weak reactivity (Zhang et al., 2006). Reaction of SO_2 gas with the lattice oxygen as in Reaction 2 seems to proceed much slower. The observation is in line with the results of experiments on dehydroxylated surfaces that show very little reactivity towards product formation, suggesting low reactivity of lattice oxygen groups (Nanayakkara et al., 2012). Absence of S-H stretch from the spectra of the v-dust under dry conditions could be due to the fact that bisulfites and bisulfates are formed in much lower quantities than in humid conditions.

3.2.2.4 Surface coverage of v-dust with SO_4^{2-} ions

The uptake of SO_2 gas on the surface of the v-dust proved to be very long and the process of conversion to H_2SO_4 was not declining for as long as the SO_2 gas was supplied, at least for the duration of the experiments. At the same time no product leaving the surface was identified. This

938 is puzzling since there seems to be no reason for continuous uptake in the absence of some kind
939 of catalytic process leading to regeneration of active sites. In this case it only makes sense that
940 sooner or later the process should come to an end. In order to evaluate a potential for further
941 uptake and conversion of SO_2 to H_2SO_4 it was decided to evaluate the surface coverage of SO_4^{2-}
942 at the end of the experiment. The amount of the product formed on the surface was quantified
943 using HPLC. A 109 mg sample of Hagavatn dust was exposed to 175 ppm of SO_2 gas for 24 hours
944 at 23°C and 30% *RH* and then flushed for 6 hours to allow complete oxidation of sulfites into
945 sulfates. The dust was then extracted in 1 mL of 1% formalin. A calibration curve was constructed
946 using Na_2SO_4 as a standard solution. The amount of SO_4^{2-} recovered was calculated at 62.79 µg
947 corresponding to 0.57 mg of SO_4^{2-} ion per 1g of Hagavatn dust. The number of molecules formed
948 after 24 hours of continuous exposure was calculated as 7.95×10^{13} molecules cm^{-2}. Considering
949 the linear trend that we observed in DRIFTS experiments, the coverage of SO_4^{2-} ions after 72
950 hours of exposure was estimated at *ca.* 2.3×10^{14} molecules cm^{-2}. To approximate whether the
951 monolayer coverage was reached it was decided to compare the amount of molecules formed on
952 the surface to its theoretical monolayer coverage.

953 The calculated value for the amount of sulfuric acid molecules necessary to form a
954 monolayer was calculated to be 4.22×10^{14} molecule cm^{-2}. This value is consistent with the
955 usually reported surface density of sorptive sites on mineral oxides, ca. 3×10^{13} - 5×10^{14} sites
956 cm^{-2} (Kulkarni and Wachs, 2002). The coverage of SO_4^{2-} ions after 72 hours of exposure was
957 estimated to be almost by a factor of 2 lower than the theoretical monolayer coverage of the
958 sample by H_2SO_4 molecules. At this point it should be noted that experimentally, the molecules
959 are not expected to pack together perfectly since the shape of the molecules and hindering
960 interactions would render some of the active sites on the surface inaccessible. Thus, the
961 experimental monolayer coverage would be assumed to be lower than the theoretical one (Hudson
962 et al., 2002), (Diaz et al., 2005).

963 The rough approximation points to the fact that the surface coverage θ after 72 hours of exposure
964 is approximately $\theta = 0.5$. Therefore, it can be concluded that there are still available sites on the
965 surface of v-dust for the conversion of SO_2 to occur and the subsequent sorption of sulfates.
966 Moreover, the process does not seem to slow down. Longer exposure times are necessary to
967 determine how the sulfate formation will behave at $\theta = 1$ when a monolayer of sulfate ions forms.

Further on, what happens after the formation of monolayer? Will the process stop, and if it continues what are the driving forces behind it?

4. CONCLUSIONS AND ATMOSPHERIC IMPLICATIONS

In this study the uptake of SO_2 gas by Icelandic v-dust was investigated. Uptake of SO_2 by v-dusts was observed even though all of them have already been exposed to SO_2 in the volcanic conduit and plume owing to their production/emission mode. Upon exposure of the v-dust to SO_2 the system reaches a steady state clearly distinct from the initial state indicating continuous consumption of SO_2 molecules. The steady state uptake coefficients for v-dusts at 30% *RH* range from $(6.6 \pm 2.6) \times 10^{-9}$ for Hagavatn to $(6.2 \pm 2.5) \times 10^{-8}$ for Mýrdalssandur. Moreover, increased uptake of the SO_2 gas in humid conditions suggests that water plays an important role in the above-mentioned processes. The DRIFTS data indicate the presence of sulfite and sulfate ions on the surface. Presence of sulfates was further detected by HPLC analysis and it was also noted that after 3 days of exposure of v-dust to 175 ppm SO_2 the surface coverage by SO_4^{2-} ions is ca. θ = 0.5, i.e. lower than the monolayer coverage suggesting that the surface of the v-dust is still active in uptake processes that are occurring on the surface. It is most likely that SO_2 gas reacts at the surface of the v-dust and forms sulfites or bisulfites, which are then converted to sulfates. Hydroxyl groups play a major role in the conversion of SO_2 gas to sulfites, while oxidizing agents in the form of active oxygen or metal centers are necessary to their conversion to sulfates. Furthermore, sulfates formed on the surface of v-dust are a stable chemisorbed species not easily desorbed even after flushing for hours in the absence of SO_2 gas.

During an episode of volcanic eruption volcanic dust will react with SO_2 gas both in subvolcanic and atmospheric environments (Renggli et al., 2019), (Schmauss and Keppler, 2014). Initially, at near-magmatic high temperatures of over 800 °C there is a compelling evidence that the adsorption of SO_2 gas is driven by diffusion of Ca^{2+} cations from the interior of the glass to its surface followed by precipitation of $CaSO_4$ (Delmelle et al., 2018). This initial stage is characterized by high concentration of gases and high density of ash particles, but is very short in duration lasting only a couple of minutes even in the case of Earth's largest explosive eruptions (Delmelle et al., 2018). The pathway is of limited importance in small and medium size eruptions and/or eruptions of volcanoes lacking a deep-seated magma chamber (Ayris et al., 2013). Subsequent cooling rapidly brings the system to the subzero temperatures (Textor et al., n.d.). At

998 ambient and low temperatures where effective diffusion of cations to the ash surface is no longer
999 possible the driving force of SO_2 adsorption is its physisorption on the surface of ash followed by
1000 chemical reaction with active sites that are available on the surface. Previous research under these
1001 conditions points out that the rate of sulfate formation is higher at low temperatures compared to
1002 room or elevated temperatures of up to 150 °C (Wu et al., 2011)·(Schmauss and Keppler, 2014).
1003 Interestingly, adsorption of SO_2 remains very strong at very low partial pressures, which confirms
1004 that adsorption is likely to happen in diluted cold parts of the plume (Schmauss and Keppler,
1005 2014). Furthermore, an increase in sulfur load on ash surfaces was observed to increase with
1006 increase of distance from the vent during 2010 Eyjafjallajökull eruption (Bagnato et al., 2013).
1007 Thus, one can expect that most of the adsorption of SO_2 gas during a medium-size volcanic
1008 eruption would happen in the horizontal umbrella part of the volcanic ash cloud. In this case it is
1009 important to use the steady state uptake coefficient to evaluate the uptake as it is better fit to
1010 describe the phenomena of the continuous process. In this research it was demonstrated that even
1011 after 3 days of exposure of natural v-dust to the SO_2 gas there are still active sites available for
1012 the reaction to take place. Therefore one can expect a v-dust particle travelling through the air to
1013 remain active to the adsorption of SO_2 gas.

1014 In order to evaluate potential impact of SO_2 adsorption on v-dust on atmosphere its
1015 atmospheric lifetime was calculated using equation 5.

1016 $$\tau_{het} = \frac{4}{\gamma c D} \quad (5)$$

1017 where γ is the uptake coefficient, c is the mean molecular velocity (m s^{-1}), and D is the
1018 volcanic dust surface area density (m^2 m^{-3}). Considering (i) concentrations of volcanic ash in a
1019 vertical column of the volcanic cloud passing over Faroe Islands located about 650 km from the
1020 Eyjafjallajökull volcano measured during its eruption on April 15 2010 ranging from 200 to 6000
1021 µg m^{-3} (Gudmundsson et al., 2012) and (ii) the *SSA* of Eyjafjallajökull dust sample of 0.75 m^2
1022 g^{-1}, D can be calculated by direct multiplication of the dust concentration and the *SSA* of the v-
1023 dust and was found to be in the range from 1.5×10^{-4} m^2 m^{-3} to 4.5×10^{-3} m^2 m^{-3} for the lower and
1024 higher ash load respectively. This leads to the calculation of lifetime of SO_2 molecule as a result
1025 of its heterogeneous loss on Eyjafjallajökull v-dust particle to 81 to 2.7 years. If we consider a
1026 higher 7.5 m^2 g^{-1} *SSA* values for Eyjafjallajökull dust obtained by Maters et al. the atmospheric

lifetime falls to 8.1 years to 99 days (Maters et al., 2016). For comparison, the lifetime of SO_2 in the atmosphere as measured over the Eastern United States in the absence of volcanic activity ranges from 15 h in summer to 65 hours in winter (Lee et al., 2011). On the base of these calculations it appears that the heterogeneous uptake of SO_2 molecule on the surface of v-dust particle is a negligible process in comparison with the gas phase oxidation by aqueous (i.e., H_2O_2) and gas-phase (i.e., OH) processes. However, in case of higher volcanic ash concentrations in the plume, for example 2.0×10^6 µg m^{-3} estimated during 1991 Pinatubo eruption (*SSA* 1.5 m^2 g^{-1} (Maters et al., 2016)) at the direct proximity to the vent (Witham et al., 2012), and considering the same uptake coefficient measured in this study for Eyjafjallajökull, calculations lead to a radically shorter lifetime of 36 hr and make heterogeneous uptake of SO_2 on volcanic dust particles equally important. Furthermore, the lifetime of SO_2 could be further decreased for volcanic particles with higher specific surface area. These calculations point out that adsorption of SO_2 on the surface of volcanic ash is most likely to happen in the part of volcanic cloud closest to the vent where ash concentration is the highest. The process of SO_2 loss due to heterogeneous reactions with v-dust particles could be further enhanced in the presence of oxidizing species (i.e., O_3, OH) and sunlight, and needs to be quantitatively evaluated.

5. ACKNOWLEDGMENTS

The authors acknowledge Mr Vincent Gaudion and Dr Mohamad Zeineddine (SAGE, IMT Lille Douai) for their assistance in the lab. We are grateful to Mr Bruno Malet and Dr Laurent Alleman (SAGE, IMT Lille Douai) for conducting the ICP-MS experiments. This work was achieved in the frame of Labex CaPPA, funded by ANR through the PIA under contract ANR-11-LABX-0005-01, and CPER CLIMIBIO project, both funded by the Hauts-de-France Regional Council and the European Regional Development Fund (ERDF). J. Lasne acknowledges support from the Labex CaPPA and CPER CLIMIBIO projects and the Hauts-de-France Regional Council for his post-doctoral fellowship.

REFERENCES

A Leed, E., Pantano, C., 2003. Computer Modeling of Water Adsorption on Silica and Silicate Glass Fracture Surfaces. Journal of Non-Crystalline Solids 325, 48–60. https://doi.org/10.1016/S0022-3093(03)00361-2

Adams, J.W., Rodriguez, D., Cox, R.A., 2005. The uptake of SO_2 on Saharan dust: a flow tube study. Atmospheric Chemistry and Physics 5, 2679–2689. https://doi.org/10.5194/acp-5-2679-2005

Alleman, L.Y., Lamaison, L., Perdrix, E., Robache, A., Galloo, J.-C., 2010. PM10 metal concentrations and source identification using positive matrix factorization and wind sectoring in a French industrial zone. Atmospheric Research 96, 612–625. https://doi.org/10.1016/j.atmosres.2010.02.008

Andreae, M., 1995. Climate Effects of Changing Atmospheric Aerosol. World Survey of Climatology. Vol. 16: Future Climates of the World, 341-392 (1995).

Arnalds, O., Dagsson-Waldhauserova, P., Olafsson, H., 2016. The Icelandic volcanic aeolian environment: Processes and impacts — A review. Aeolian Research 20, 176–195. https://doi.org/10.1016/j.aeolia.2016.01.004

Ayris, P.M., Lee, A.F., Wilson, K., Kueppers, U., Dingwell, D.B., Delmelle, P., 2013. SO2 sequestration in large volcanic eruptions: High-temperature scavenging by tephra. Geochimica et Cosmochimica Acta 110, 58–69. https://doi.org/10.1016/j.gca.2013.02.018

Bagnato, E., Aiuppa, A., Bertagnini, A., Bonadonna, C., Cioni, R., Pistolesi, M., Pedone, M., Hoskuldsson, A., 2013. Scavenging of sulphur, halogens and trace metals by volcanic ash: The 2010 Eyjafjallajökull eruption. Geochimica et Cosmochimica Acta 103, 138–160. https://doi.org/10.1016/j.gca.2012.10.048

Baltrusaitis, J., Cwiertny, D.M., Grassian, V.H., 2007. Adsorption of sulfur dioxide on hematite and goethite particle surfaces. Phys. Chem. Chem. Phys. 9, 5542–5554. https://doi.org/10.1039/B709167B

Baratoux, D., Mangold, N., Arnalds, O., Bardintzeff, J.-M., Platevoet, B., Grégoire, M., Pinet, P., 2011. Volcanic Sand in Iceland: Diverse origins of aeolian sand deposits revealed at Dyngjusandur and Lambahraun, Iceland. Earth Surface Processes and Landforms 36, 1789–1808. https://doi.org/10.1002/esp.2201

Brasseur, G.P., Granier, C., Walters, S., 1990. Future changes in stratospheric ozone and the role of heterogeneous chemistry. Nature 348, 626–628. https://doi.org/10.1038/348626a0

Clague, D.A., Denlinger, R.P., 1994. Role of olivine cumulates in destabilizing the flanks of Hawaiian volcanoes. Bull Volcanol 56, 425–434. https://doi.org/10.1007/BF00302824

Crowley, J.N., Ammann, M., Cox, R.A., Hynes, R.G., Jenkin, M.E., Mellouki, A., Rossi, M.J., Troe, J., Wallington, T.J., 2010. Evaluated kinetic and photochemical data for atmospheric chemistry: Volume V – heterogeneous reactions on solid substrates. Atmos. Chem. Phys. 10, 9059–9223. https://doi.org/10.5194/acp-10-9059-2010

Dagsson-Waldhauserova, P., Arnalds, O., Olafsson, H., 2014. Long-term variability of dust events in Iceland (1949–2011). Atmos. Chem. Phys. 14, 13411–13422. https://doi.org/10.5194/acp-14-13411-2014

Datta, A., Cavell, R.G., Tower, R.W., George, Z.M., 1985. Claus catalysis. 1. Adsorption of SO/sub 2/ on the alumina catalyst studed by FTIR and EPR spectroscopy. J. Phys. Chem.; (United States) 89:3. https://doi.org/10.1021/j100249a014

Deegan, F.M., 2010. Processes of Magma-crust Interaction Insights from Geochemistry and Experimental Petrology. Acta Universitatis Upsaliensis, Uppsala.
Delmelle, P., Wadsworth, F.B., Maters, E.C., Ayris, P.M., 2018. High Temperature Reactions Between Gases and Ash Particles in Volcanic Eruption Plumes. Reviews in Mineralogy and Geochemistry 84, 285–308. https://doi.org/10.2138/rmg.2018.84.8
Diaz, L., Liauw, C.M., Edge, M., Allen, N.S., McMahon, A., Rhodes, N., 2005. Investigation of factors affecting the adsorption of functional molecules onto gel silicas. 1. Flow microcalorimetry and infrared spectroscopy. J Colloid Interface Sci 287, 379–387. https://doi.org/10.1016/j.jcis.2004.09.039
Dordevic, D., Tošić, I., Sakan, S., Petrovic, S., Đuričić-Milanković, J., Finger, D., Waldhauserova, P., 2019. Can Volcanic Dust Suspended From Surface Soil and Deserts of Iceland Be Transferred to Central Balkan Similarly to African Dust (Sahara)? Frontiers in Earth Science 7, 142. https://doi.org/10.3389/feart.2019.00142
Durant, A.J., Bonadonna, C., Horwell, C.J., 2010. Atmospheric and Environmental Impacts of Volcanic Particulates. Elements 6, 235–240.
Durant, A.J., Shaw, R.A., Rose, W.I., Mi, Y., Ernst, G.G.J., 2008. Ice nucleation and overseeding of ice in volcanic clouds. Journal of Geophysical Research: Atmospheres 113. https://doi.org/10.1029/2007JD009064
Farges, F., Keppler, H., Flank, A.M., Lagarde, P., 2009. Sulfur K-edge XANES study of S sorbed onto volcanic ashes. Journal of Physics: Conference Series 190, 012177. https://doi.org/10.1088/1742-6596/190/1/012177
Finlayson-Pitts, B.J., Jr, J.N.P., 1999. Chemistry of the Upper and Lower Atmosphere: Theory, Experiments, and Applications. Elsevier.
Gislason, S.R., Hassenkam, T., Nedel, S., Bovet, N., Eiriksdottir, E.S., Alfredsson, H.A., Hem, C.P., Balogh, Z.I., Dideriksen, K., Oskarsson, N., Sigfusson, B., Larsen, G., Stipp, S.L.S., 2011. Characterization of Eyjafjallajökull volcanic ash particles and a protocol for rapid risk assessment. PNAS 108, 7307–7312. https://doi.org/10.1073/pnas.1015053108
Goodman, A.L., Li, P., Usher, C.R., Grassian, V.H., 2001. Heterogeneous Uptake of Sulfur Dioxide On Aluminum and Magnesium Oxide Particles. J. Phys. Chem. A 105, 6109–6120. https://doi.org/10.1021/jp004423z
Groot Zwaaftink, C.D., Arnalds, Ó., Dagsson-Waldhauserova, P., Eckhardt, S., Prospero, J.M., Stohl, A., 2017. Temporal and spatial variability of Icelandic dust emissions and atmospheric transport. Atmospheric Chemistry and Physics 17, 10865–10878. https://doi.org/10.5194/acp-17-10865-2017
Gudmundsson, M.T., Thordarson, T., Höskuldsson, Á., Larsen, G., Björnsson, H., Prata, F.J., Oddsson, B., Magnússon, E., Högnadóttir, T., Petersen, G.N., Hayward, C.L., Stevenson, J.A., Jónsdóttir, I., 2012. Ash generation and distribution from the April-May 2010 eruption of Eyjafjallajökull, Iceland. Scientific Reports 2, 572. https://doi.org/10.1038/srep00572
Hair, M.L., 1975. Hydroxyl groups on silica surface. Journal of Non-Crystalline Solids, Glass Surfaces 19, 299–309. https://doi.org/10.1016/0022-3093(75)90095-2
Harris, E., Sinha, B., Foley, S., Crowley, J.N., Borrmann, S., Hoppe, P., 2012. Sulfur isotope fractionation during heterogeneous oxidation of SO₂ on mineral dust. Atmospheric Chemistry and Physics 12, 4867–4884. https://doi.org/10.5194/acp-12-4867-2012

1143 Highwood, E.-J., Stevenson, D.S., 2003. Atmospheric impact of the 1783-1784 Laki Eruption:
1144 Part II Climatic effect of sulphate aerosol. Atmospheric Chemistry and Physics 3, 1177–
1145 1189.
1146 Huang, L., Zhao, Y., Li, H., Chen, Z., 2015. Kinetics of Heterogeneous Reaction of Sulfur
1147 Dioxide on Authentic Mineral Dust: Effects of Relative Humidity and Hydrogen
1148 Peroxide. Environ. Sci. Technol. 49, 10797–10805.
1149 https://doi.org/10.1021/acs.est.5b03930
1150 Hudson, P.K., Zondlo, M.A., Tolbert, M.A., 2002. The Interaction of Methanol, Acetone, and
1151 Acetaldehyde with Ice and Nitric Acid-Doped Ice: Implications for Cirrus Clouds. J.
1152 Phys. Chem. A 106, 2882–2888. https://doi.org/10.1021/jp012718m
1153 Huthwelker, T., Ammann, M., Peter, T., 2006. The Uptake of Acidic Gases on Ice. Chemical
1154 Reviews 106, 1375–1444. https://doi.org/10.1021/cr020506v
1155 Ibrahim, S., Romanias, M.N., Alleman, L.Y., Zeineddine, M.N., Angeli, G.K., Trikalitis, P.N.,
1156 Thevenet, F., 2018. Water Interaction with Mineral Dust Aerosol: Particle Size and
1157 Hygroscopic Properties of Dust. ACS Earth Space Chem. 2, 376–386.
1158 https://doi.org/10.1021/acsearthspacechem.7b00152
1159 Icelandic Volcanoes [WWW Document], n.d. URL http://icelandicvolcanos.is/?volcano=EYJ#
1160 (accessed 2.20.19).
1161 Jiang, B.Q., Wu, Z.B., Liu, Y., Lee, S.C., Ho, W.K., 2010. DRIFT Study of the SO2 Effect on
1162 Low-Temperature SCR Reaction over Fe−Mn/TiO2. J. Phys. Chem. C 114, 4961–4965.
1163 https://doi.org/10.1021/jp907783g
1164 Joshi, N., Romanias, M.N., Riffault, V., Thevenet, F., 2017. Investigating water adsorption onto
1165 natural mineral dust particles: Linking DRIFTS experiments and BET theory. Aeolian
1166 Research 27, 35–45. https://doi.org/10.1016/j.aeolia.2017.06.001
1167 Judeikis, H.S., Stewart, T.B., 1976. Laboratory measurement of SO2 deposition velocities on
1168 selected building materials and soils. Atmospheric Environment (1967) 10, 769–776.
1169 https://doi.org/10.1016/0004-6981(76)90078-0
1170 Kulkarni, D., Wachs, I.E., 2002. Isopropanol oxidation by pure metal oxide catalysts: number of
1171 active surface sites and turnover frequencies. Applied Catalysis A: General 237, 121–137.
1172 https://doi.org/10.1016/S0926-860X(02)00325-3
1173 Langmann, B., 2013. Volcanic Ash versus Mineral Dust: Atmospheric Processing and
1174 Environmental and Climate Impacts [WWW Document]. International Scholarly
1175 Research Notices. https://doi.org/10.1155/2013/245076
1176 Langmann, B., Zakšek, K., Hort, M., 2010. Atmospheric distribution and removal of volcanic ash
1177 after the eruption of Kasatochi volcano: A regional model study. Journal of Geophysical
1178 Research: Atmospheres 115. https://doi.org/10.1029/2009JD013298
1179 Lasne, J., Romanias, M.N., Thevenet, F., 2018. Ozone Uptake by Clay Dusts under
1180 Environmental Conditions. ACS Earth Space Chem. 2, 904–914.
1181 https://doi.org/10.1021/acsearthspacechem.8b00057
1182 Lee, C., Martin, R.V., Donkelaar, A. van, Lee, H., Dickerson, R.R., Hains, J.C., Krotkov, N.,
1183 Richter, A., Vinnikov, K., Schwab, J.J., 2011. SO2 emissions and lifetimes: Estimates
1184 from inverse modeling using in situ and global, space-based (SCIAMACHY and OMI)
1185 observations. Journal of Geophysical Research: Atmospheres 116.
1186 https://doi.org/10.1029/2010JD014758
1187 Li, L., Chen, Z.M., Zhang, Y.H., Zhu, T., Li, J.L., Ding, J., 2006. Kinetics and mechanism of
1188 heterogeneous oxidation of sulfur dioxide by ozone on surface of calcium carbonate.

Atmospheric Chemistry and Physics Discussions 6, 579–613. https://doi.org/10.5194/acpd-6-579-2006
Lo, J.M.H., Ziegler, T., Clark, P.D., 2010. SO2 Adsorption and Transformations on γ-Al2O3 Surfaces: A Density Functional Theory Study. J. Phys. Chem. C 114, 10444–10454. https://doi.org/10.1021/jp910895g
Massman, W.J., 1998. A review of the molecular diffusivities of H2O, CO2, CH4, CO, O3, SO2, NH3, N2O, NO, and NO2 in air O2 and N2 near STP [WWW Document]. Atmospheric Environment. URL https://eurekamag.com/research/008/072/008072627.php (accessed 11.5.18).
Maters, E.C., Delmelle, P., Rossi, M.J., Ayris, P.M., 2017. Reactive Uptake of Sulfur Dioxide and Ozone on Volcanic Glass and Ash at Ambient Temperature. J. Geophys. Res.-Atmos. 122, 10077–10088. https://doi.org/10.1002/2017JD026993
Maters, E.C., Delmelle, P., Rossi, M.J., Ayris, P.M., Bernard, A., 2016. Controls on the surface chemical reactivity of volcanic ash investigated with probe gases. Earth Planet. Sci. Lett. 450, 254–262. https://doi.org/10.1016/j.epsl.2016.06.044
Michigami, Y., Ueda, K., 1994. Sulphite stabilizer in ion chromatography. Journal of Chromatography A 663, 255–258. https://doi.org/10.1016/0021-9673(94)85252-9
Moroni, B., Arnalds, O., Dagsson-Waldhauserová, P., Crocchianti, S., Vivani, R., Cappelletti, D., 2018. Mineralogical and Chemical Records of Icelandic Dust Sources Upon Ny-Ålesund (Svalbard Islands). Front. Earth Sci. 6. https://doi.org/10.3389/feart.2018.00187
Nanayakkara, C.E., Pettibone, J., Grassian, V.H., 2012. Sulfur dioxide adsorption and photooxidation on isotopically-labeled titanium dioxide nanoparticle surfaces: roles of surface hydroxyl groups and adsorbed water in the formation and stability of adsorbed sulfite and sulfate. Phys. Chem. Chem. Phys. 14, 6957–6966. https://doi.org/10.1039/C2CP23684B
Ovadnevaite, J., Ceburnis, D., Plauskaite-Sukiene, K., Modini, R., Dupuy, R., Rimselyte, I., Ramonet, M., Kvietkus, K., Ristovski, Z., Berresheim, H., O'Dowd, C.D., 2009. Volcanic sulphate and arctic dust plumes over the North Atlantic Ocean. Atmospheric Environment 43, 4968–4974. https://doi.org/10.1016/j.atmosenv.2009.07.007
Reactions on Mineral Dust - Chemical Reviews (ACS Publications) [WWW Document], n.d. URL https://pubs.acs.org/doi/abs/10.1021/cr020657y (accessed 2.8.18).
Renggli, C., King, P., W. Henley, R., Guagliardo, P., McMorrow, L., Middleton, J., Turner, M., 2019. An experimental study of SO2 reactions with silicate glasses and supercooled melts in the system anorthite–diopside–albite at high temperature. Contributions to Mineralogy and Petrology 174. https://doi.org/10.1007/s00410-018-1538-2
Romanias, M.N., El Zein, A., Bedjanian, Y., 2012. Heterogeneous Interaction of H2O2 with TiO2 Surface under Dark and UV Light Irradiation Conditions. J. Phys. Chem. A 116, 8191–8200. https://doi.org/10.1021/jp305366v
Romanías, M.N., Ourrad, H., Thévenet, F., Riffault, V., 2016. Investigating the Heterogeneous Interaction of VOCs with Natural Atmospheric Particles: Adsorption of Limonene and Toluene on Saharan Mineral Dusts. J. Phys. Chem. A 120, 1197–1212. https://doi.org/10.1021/acs.jpca.5b10323
Romanias, M.N., Zeineddine, M.N., Gaudion, V., Lun, X., Thevenet, F., Riffault, V., 2016. Heterogeneous Interaction of Isopropanol with Natural Gobi Dust. Environ. Sci. Technol. 50, 11714–11722. https://doi.org/10.1021/acs.est.6b03708
Schmauss, D., Keppler, H., 2014. Adsorption of sulfur dioxide on volcanic ashes. American Mineralogist 99, 1085–1094. https://doi.org/10.2138/am.2014.4656

Schmidt, A., Witham, C.S., Theys, N., Richards, N.A.D., Thordarson, T., Szpek, K., Feng, W., Hort, M.C., Woolley, A.M., Jones, A.R., Redington, A.L., Johnson, B.T., Hayward, C.L., Carslaw, K.S., 2014. Assessing hazards to aviation from sulfur dioxide emitted by explosive Icelandic eruptions. J. Geophys. Res. Atmos. 119, 2014JD022070. https://doi.org/10.1002/2014JD022070

Shang, J., Li, J., Zhu, T., 2010. Heterogeneous reaction of SO2 on TiO2 particles. Sci. China Chem. 53, 2637–2643. https://doi.org/10.1007/s11426-010-4160-3

Stevenson, D.S., Johnson, C.E., Highwood, E.J., Gauci, V., Collins, W.J., Derwent, R.G., 2003. Atmospheric impact of the 1783–1784 Laki eruption: Part I Chemistry modelling. Atmos. Chem. Phys. 3, 487–507. https://doi.org/10.5194/acp-3-487-2003

Tambora and the "Year Without a Summer" of 1816 [WWW Document], 2016. . Institute of Geography. URL http://www.geography.unibe.ch/services/geographica_bernensia/online/gb2016g9001/index_eng.html (accessed 5.17.18).

Tamura, H., Mita, K., Tanaka, A., Ito, M., 2001. Mechanism of Hydroxylation of Metal Oxide Surfaces. Journal of Colloid and Interface Science 243, 202–207. https://doi.org/10.1006/jcis.2001.7864

Tang, M.J., Cox, R.A., Kalberer, M., 2014. Compilation and evaluation of gas phase diffusion coefficients of reactive trace gases in the atmosphere: volume 1. Inorganic compounds. Atmospheric Chemistry and Physics 14, 9233–9247. https://doi.org/10.5194/acp-14-9233-2014

Textor, C., Graf, H.-F., Herzog, M., Oberhuber, J.M., n.d. Injection of gases into the stratosphere by explosive volcanic eruptions. Journal of Geophysical Research: Atmospheres 108. https://doi.org/10.1029/2002JD002987

Thordarson, T., Larsen, G., 2007. Volcanism in Iceland in historical time: Volcano types, eruption styles and eruptive history. Journal of Geodynamics - J GEODYNAMICS 43, 118–152. https://doi.org/10.1016/j.jog.2006.09.005

Ullerstam, M., Vogt, R., Langer, S., Ljungstrom, E., 2002. The kinetics and mechanism of SO2 oxidation by O-3 on mineral dust. Phys. Chem. Chem. Phys. 4, 4694–4699. https://doi.org/10.1039/b203529b

Usher, C.R., Al-Hosney, H., Carlos-Cuellar, S., Grassian, V.H., 2002. A laboratory study of the heterogeneous uptake and oxidation of sulfur dioxide on mineral dust particles. J.-Geophys.-Res. 107, 4713. https://doi.org/10.1029/2002JD002051

Vernier, J.-P., Fairlie, T.D., Deshler, T., Natarajan, M., Knepp, T., Foster, K., Wienhold, F.G., Bedka, K.M., Thomason, L., Trepte, C., n.d. In situ and space-based observations of the Kelud volcanic plume: The persistence of ash in the lower stratosphere. Journal of Geophysical Research: Atmospheres 121, 11,104-11,118. https://doi.org/10.1002/2016JD025344

Vogel, A., Diplas, S., Durant, A.J., Azar, A.S., Sunding, M.F., Rose, W.I., Sytchkova, A., Bonadonna, C., Krüger, K., Stohl, A., 2017. Reference data set of volcanic ash physicochemical and optical properties. Journal of Geophysical Research: Atmospheres 122, 9485–9514. https://doi.org/10.1002/2016JD026328

Wang, T., Liu, Y., Deng, Y., Fu, H., Zhang, L., Chen, J., 2018a. Emerging investigator series: heterogeneous reactions of sulfur dioxide on mineral dust nanoparticles: from single component to mixed components. Environ. Sci.: Nano 5, 1821–1833. https://doi.org/10.1039/C8EN00376A

Wang, T., Liu, Y., Deng, Y., Fu, H., Zhang, L., Chen, J.-M., 2018b. Adsorption of SO 2 on mineral dust particles influenced by atmospheric moisture. Atmospheric Environment 191. https://doi.org/10.1016/j.atmosenv.2018.08.008

Witham, C., Webster, H., Hort, M., Jones, A., Thomson, D., 2012. Modelling concentrations of volcanic ash encountered by aircraft in past eruptions. Atmospheric Environment, Volcanic ash over Europe during the eruption of Eyjafjallajöekull on Iceland, April-May 2010 48, 219–229. https://doi.org/10.1016/j.atmosenv.2011.06.073

Witham, C.S., Oppenheimer, C., Horwell, C.J., 2005. Volcanic ash-leachates: a review and recommendations for sampling methods. Journal of Volcanology and Geothermal Research 141, 299–326. https://doi.org/10.1016/j.jvolgeores.2004.11.010

Wu, L.Y., Tong, S.R., Wang, W.G., Ge, M.F., 2011. Effects of temperature on the heterogeneous oxidation of sulfur dioxide by ozone on calcium carbonate. Atmospheric Chemistry and Physics 11, 6593–6605. https://doi.org/10.5194/acp-11-6593-2011

Zhang, X., Zhuang, G., Chen, J., Wang, Y., Wang, X., An, Z., Zhang, P., 2006. Heterogeneous Reactions of Sulfur Dioxide on Typical Mineral Particles. J. Phys. Chem. B 110, 12588–12596. https://doi.org/10.1021/jp0617773

Zhang, Y., Tong, S., Ge, M., Jing, B., Hou, S., Tan, F., Chen, Y., Guo, Y., Wu, L., 2018. The influence of relative humidity on the heterogeneous oxidation of sulfur dioxide by ozone on calcium carbonate particles. Sci. Total Environ. 633, 1253–1262. https://doi.org/10.1016/j.scitotenv.2018.03.288

Zhang, Z., Ewing, G.E., 2002. Infrared spectroscopy of SO2 aqueous solutions. Spectrochim Acta A Mol Biomol Spectrosc 58, 2105–2113.

Zhou, L., Wang, W., Gai, Y., Ge, M., 2014. Knudsen cell and smog chamber study of the heterogeneous uptake of sulfur dioxide on Chinese mineral dust. Journal of Environmental Sciences 26, 2423–2433. https://doi.org/10.1016/j.jes.2014.04.005

Zuo, Y., Chen, H., 2003. Simultaneous determination of sulfite, sulfate, and hydroxymethanesulfonate in atmospheric waters by ion-pair HPLC technique. Talanta 59, 875–881. https://doi.org/10.1016/S0039-9140(02)00647-1